*Geochimica et Cosmochimica Acta* Vol. 57, pp. 1837–1856


0016-7037/93/$6.00 + .00

# Sm-Nd isotopic evidence for the provenance of sediments from the Adelaide Fold Belt and southeastern Australia with implications for episodic crustal addition

SIMON TURNER,* JOHN FODEN, MIKE SANDIFORD, and DAVID BRUCE
Department of Geology and Geophysics, University of Adelaide, GPO Box 498, SA 5001, Australia

(*Received June* 19, 1992; *accepted in revised form October* 24, 1992)

**Abstract**—In South Australia, Late Proterozoic and Cambrian sediments were deposited in basins formed within Archaean to Early Mid-Proterozoic basement. These sequences were subsequently deformed and uplifted by the Cambro-Ordovician Delamerian Orogeny to form the Adelaide Fold Belt. In using the Adelaide Fold Belt to address models for lithospheric evolution, it is necessary to understand the mechanisms of basin formation and whether the sequences merely reflect reworking of existing cratonic material or if there were new crustal additions. This study presents geochemical and isotopic data on the sediments and basement rocks to complement existing data on the Delamerian igneous rocks as a means of investigating these questions.

The data reveal that the Archaean-Mid Proterozoic basement rocks of the Gawler Craton have Nd depleted mantle model ages which average about 2.6 Ga and $\epsilon$Nd values at 800 Ma in the range −9 to −24 or at 500 Ma from −11 to −28. The Late Proterozoic Adelaidean sediments, however, have an average model age of 1.9 Ga and initial $\epsilon$Nd values in the range −5 to −11. The sequence can be divided into lowermost rift-phase sediments derived from erosion of local Gawler Craton material, and a subsequent, widely distributed, thermal-sag-phase sedimentation whose isotopic signature is not compatible with the basement. This implies that a more primitive or juvenile source was accessed via broadening of the provenance region. The Cambrian sediments have slightly older model ages (2.1 Ga) and lower $\epsilon$Nd (−9 to −13) and can be interpreted as mixtures of basement and reworked Adelaidean detritus.

The Early Palaeozoic sedimentary sequences of the Lachlan Fold Belt to the east have isotopic compositions very like the South Australian Late Proterozoic and Cambrian sequences. They have an average model age of 1.85 Ma but much higher $K_2O/Na_2O$. This indicates that the widespread flysch of eastern Australia is the result of recycling of the Late Proterozoic and Cambrian sediments by erosion of the Adelaide Fold Belt, with some modification by the mixture of the Cambro-Ordovician mafic and felsic magmatic rocks in this orogen.

Our data suggest regional, intracontinental, crustal evolution combined with recycling of older crustal material with new additions from the mantle during orogenesis and, to a lesser extent, episodes of extension and sedimentation.

## INTRODUCTION

MODELS FOR THE EVOLUTION of the continental lithosphere have two endmember camps. The steady-state model advocated by ARMSTRONG (1981, 1991) proposes very early earth differentiation into a constant volume crust and depleted mantle with subsequent geological history principally involving recycling. An alternative view, maintained by many workers (e.g., DEWEY and WINDLEY, 1981; ALLÈGRE, 1982; REYMER and SCHUBERT, 1984; TAYLOR and MCLENNAN, 1985), is that the continents have grown steadily or episodically throughout geological time. Orogenic belts are possible sites of continental accretion and growth, and typically these involve thick sedimentary sequences subsequently deformed during an orogenic event involving metamorphism and magmatism. Deciding whether the evolution of such orogenic belts involve fresh additions from the mantle, or alternatively simply record crustal reworking is an important first order step in constraining current debates on crustal growth models.

In this contribution, we present isotopical and geochemical data on sediments and their potential source rocks from the Late Proterozoic-Cambrian Adelaide Fold Belt with the aim of constraining their provenance regions and thereby assessing lithospheric evolution in this orogen.

## THE ADELAIDE FOLD BELT, SOUTH AUSTRALIA

The intracratonic Adelaide Fold Belt forms part of one of the largest and best preserved Late Proterozoic-Early Cambrian fold belts in the world. It extends through most of the length of South Australia with equivalent sequences in western Tasmania (e.g., WILLIAMS, 1978) and in north Victoria Land, Antarctica (e.g., LAIRD and GRINDLEY, 1982), leading various authors (e.g., BALLIE, 1985) to propose that an originally contiguous fold belt formed the then eastern margin of Gondwanaland.

In South Australia, Archaean to mid-Proterozoic orogenic sequences of the Gawler Craton are basement to thick sequences of sediments deposited during Late Proterozoic and Early Cambrian time (Figs. 1 and 2). On Eyre Peninsula, the Archaean to Mid-Proterozoic rocks of the Gawler Craton show a history punctuated by three principle episodes of magmatism and deformation, interspersed by periods of sedimentation (see WEBB et al., 1986; FANNING et al., 1988, and references therein for detailed discussions of Gawler

* *Present address:* Department of Earth Sciences, Open University, Milton Keynes, MK7 6AA, England.

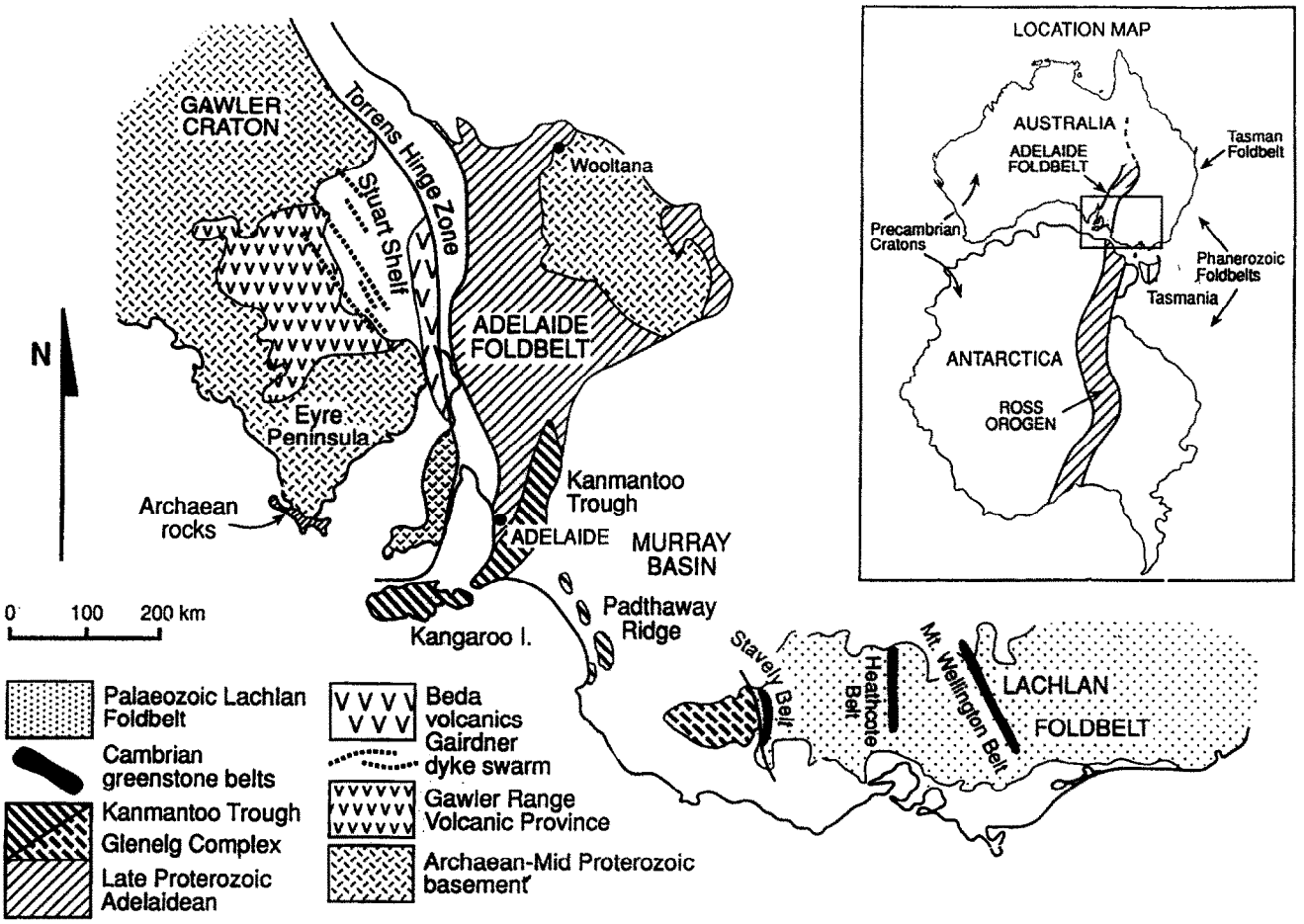


FIG. 1. Map of southeastern Australia showing the Archaean to Mid-Proterozoic Gawler Craton, the Late Proterozoic Adelaide Fold Belt, including the Cambrian Kanmantoo Trough in the southern Adelaide Fold Belt, and the Palaeozoic Lachlan Fold Belt to the east. The insert location map shows the Gondwanan correlation with Antarctica.

Craton stratigraphy, relationships, and geochronology). Multiple deformed paragneisses were intruded by mafic and felsic magmas during the 2500–2300 Ma Sleafordian Orogeny. Subsequently, the 1820–1580 Ma Kimban Orogeny deformed younger sediments and magmatic rocks of the Hutchison Group and Lincoln Complex. Renewed felsic magmatism, sedimentation, and minor deformation mark the time of cratonization at around 1580–1400 Ma (Wartakan Event).

The Late Proterozoic sediments of the Adelaide Fold Belt (see PREISS, 1987, for review) were deposited in shelf to near-shelf environments developed in probable intracratonic rifts in this basement material. JENKINS (1990), following models for the thermal evolution of extensional basins (MCKENZIE, 1978), related these sequences in the northern half of the fold belt to cycles showing a classic Steer's Head morphology, each containing an early restricted, rift-phase succeeded by a laterally extensive thermal-sag-phase. Just preceding the earliest stages of sedimentation are the mafic dykes of the ~1000 Ma Gairdner Dyke Swarm, whilst the early, evaporite-bearing Callanna Group sedimentation was accompanied by the ~900 Ma, continental-flood-basalt style, Wooltana Volcanics (CRAWFORD and HILYARD, 1990). The subsequent and laterally extensive sedimentation of the Burra, Umberatana, and Wilpena Groups is generally characterized by shallow water deposits and a general absence of volcanic activity.

Sedimentation continued into the Cambrian and, in the southern Adelaide Fold Belt, the Cambrian Normanville Group hosts the mafic Truro Volcanics (FORBES et al., 1972; VAN DER STELDT, 1990). Overlying either the Adelaidean or the Normanville Group, which is only locally preserved, the Cambrian Kanmantoo Group consists of rapidly deposited flysch-like sediments (e.g., PREISS, 1987). The intercalation of the Normanville Group with mafic volcanics and the sudden influx of the thick turbiditic sequences of the Kanmantoo Group suggest renewed extension, and these Cambrian sediments may have been deposited in a developing rift (VON DER BORCH, 1980). Recent zircon dating on a tuffaceous layer in the upper part of the Normanville Group places the beginning of this last sedimentation episode at ~526 Ma (COOPER et al., 1992). Very rapid sedimentation is implied because the Kanmantoo sequences were evidently buried to 10–15 km depth, metamorphosed and intruded by granitic magmas by 520–516 Ma (FODEN et al., 1993b).

The Adelaidean, Normanville, and Kanmantoo sedimen-

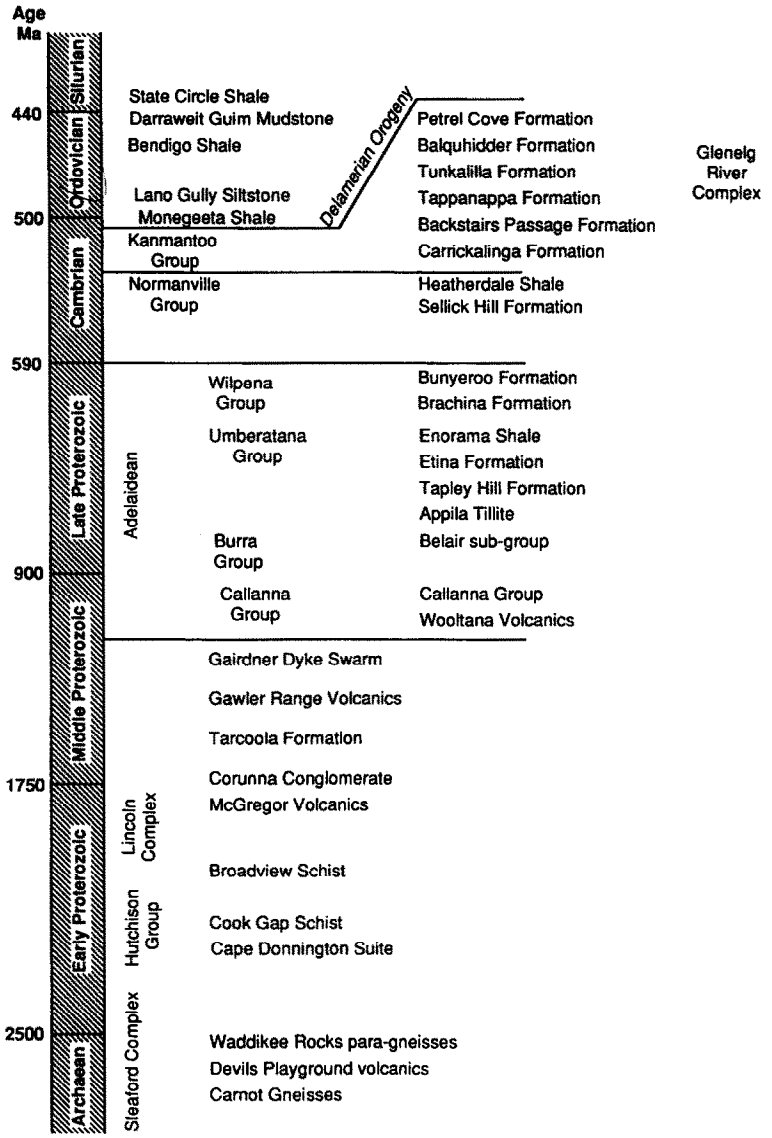


FIG. 2. Stratigraphic table listing the lithologies sampled in this study and their relative stratigraphic relationships.

tary sequences were subsequently deformed by the Cambro-Ordovician Delamerian Orogeny (THOMPSON, 1969; DAILY et al., 1976). In the southerly exposed sections of the fold belt, the Delamerian Orogeny resulted in complex polyphase deformation and Buchan-style metamorphism (e.g., MANCKTELOW, 1979; SANDIFORD et al., 1990, 1992). Magmatic activity, whilst not voluminous, occurred throughout much of the history of the fold belt (FODEN et al., 1990; TURNER and FODEN, 1990) from syn-sedimentary mafic dykes and volcanics marking periods of maximum extension to the mafic and silicic activity (orogenic I- and S-type granites and a late-orogenic bimodal suite of A-type granites and mafic intrusives) which spanned the compression of the Delamerian Orogeny (FODEN et al., 1993a,b; SANDIFORD et al., 1992; TURNER et al., 1992a).

The Late Proterozoic Adelaidean sedimentary sequences have usually been interpreted to have been derived from the Gawler Craton to the west and similar materials to the northeast (e.g., PREISS, 1987). However, the flysch-like sediments of the Cambrian Kanmantoo Group are also the most highly metamorphosed and deformed, and this unusual feature has recently led to critical re-appraisals of the tectonic history of the fold belt and the suggestion that the Kanmantoo Group may be allochthonous (e.g., JENKINS, 1986, 1990). Investigations in western Victoria (TURNER et al., 1992b) suggest correlation of the tectonic evolution of the Glenelg River Complex (Fig. 1) with that of the Kanmantoo in South Australia.

Delamerian deformation involved thrusting and crustal thickening (MANCKTELOW, 1979; SANDIFORD et al., 1990). Metamorphic grades in the Kanmantoo reach upper amphibolite grade with local development of kyanite-sillimanite assemblages. SANDIFORD et al. (1990) showed that these currently exposed assemblages formed at around 3–5 kbar (10–

17 km depth) via advection of heat from syntectonic magmas emplaced around 520–490 Ma (FODEN et al., 1993b). Given that these rocks are exposed at the same structural level as undeformed, high-level silicic granites and volcanics (TURNER et al., 1992a) intruded at 486 Ma (FODEN et al., 1992b), this suggests a rapid unroofing (~10 km) of the orogen and a possible origin for the extensive Ordovician turbidite sequences of the Lachlan Fold Belt (e.g., CAS, 1983) to the east (Fig. 1).

## OBJECTIVES

This study was initiated with the aim of constraining several endmember models for the evolution of the Adelaide Fold Belt, these in turn having implications for crustal evolution and growth models. Specifically, do the Adelaidean sedimentary sequences merely reflect reworking of the cratonic material to the west on Eyre Peninsula or was there crustal growth via synchronous, new additions from the mantle, in which case these mantle additions may be reflected in the chemical/isotopic signature of sedimentary detritus? Similarly, does the Kanmantoo Group reflect further erosion from the craton, or reworking and redeposition of the Adelaidean sequences? Alternatively, was the Kanmantoo derived from a completely different source, such as an emerging foreland to the east? Again there may have been crustal growth contemporary with Kanmantoo deposition and this may be reflected in its signature. Taking a broader perspective, are sediments from contiguous parts of Antarctica and the Glenelg River Complex equivalent to either the Kanmantoo or the Adelaidean, and do the extensive Ordovician turbidite sequences of the Lachlan Fold Belt represent material eroded off a Delamerian mountain range?

## APPROACH

### Sampling

Geochemical and isotopic data can be powerful in discriminating the sources of igneous, and perhaps to a lesser extent, sedimentary rocks. In the later case, the robustness of the Sm-Nd isotopic system, even through sedimentary and metamorphic cycles, enables it to be used as a tracer of the source materials of sedimentary rocks (MCCULLOCH and WASSERBURG, 1978; ALLÈGRE and ROUSSEAU, 1984; MILLER et al., 1986). Although caution must be exercised in interpretation (e.g., ARNDT and GOLDSTEIN, 1987; AWWILLER and MACK, 1991), in general the Sm/Nd and $^{143}Nd/^{144}Nd$ ratios of a sedimentary rock reflect the average of the source rocks in its provenance region, whilst its Nd depleted mantle model age $T_{DM}$ reflects the average time of the separation of this terrane from the mantle, i.e., its crustal residency time (e.g., MCCULLOCH and WASSERBURG, 1978). Shales are usually used in these studies because, being well mixed and distal, they are likely to provide a good average sampling of a provenance region. Restricting the study to shales may help to avoid the effects of sedimentary sorting and fractionation described by FROST and WINSTON (1987), MCLENNAN et al. (1989) and ZHAO et al. (1992). Accordingly, as a means of tackling the questions previously outlined, we have selected a series of shale-rich sediments from the Adelaidean and Kanmantoo sequences as well as several from the Glenelg River Complex, Antarctica, and the Early Palaeozoic turbidite sequences of the Lachlan Fold Belt for Sm-Nd analysis.

The occurrence of an impact ejecta horizon within the Bunyeroo Formation of the Adelaidean sequence (GOSTIN et al., 1986) provides a unique timeline within an extensive sedimentary formation, and so samples were taken 40 cm below the ejecta horizon from four localities extending over ~1000 km in order to investigate possible provenance variations along the basin. In addition, a selection of mafic and felsic plutonic and volcanic rocks were taken from the Archaean and Lower to Mid-Proterozoic of the Gawler Craton in order to characterize these potential source materials. Several metasediments were also sampled from the Gawler Craton as being potentially representative of the average cratonic composition at their time of deposition. An outline of the relevant stratigraphy is presented in Fig. 2.

### Analytical Methods

Major and trace element concentrations were determined by Philips PW148 XRF and $^{87}Rb/^{86}Sr$ was calculated from Rb and Sr analyses obtained from an extended measurement routine. Thermal ionization mass spectrometry was used to analyse the rare earth elements (REE), Nd and Sm concentrations, and Nd and Sr isotopic compositions. The concentrations were determined on 100 mg of sample which was dissolved and mixed with a multielement REE or $^{150}Nd$-$^{147}Sm$ tracer using HF and HF-$HNO_3$ in a PFA vial. This was converted to chloride using 6N HCl. Neodymum, samarium and strontium were separated using a two-stage cation exchange column procedure, essentially the same as that described by RICHARD et al. (1976). The resulting Nd, Sm, and Sr samples were loaded onto double Ta-Re rhenium and single tantalum filaments, respectively, and analysed for their isotopic compositions on a Finnigan MAT 261 solid source mass spectrometer. Data blocks of ten scans were run until acceptable within-run statistics were achieved (8–15 blocks for Sr with fixed double collector and 15–25 blocks for Nd with single collector). All Sr and Nd isotopic ratios were corrected for mass fractionation by normalizing $^{88}Sr/^{86}Sr$ to 8.3752 and $^{146}Nd/^{144}Nd$ to 0.7219. Isotopic ratio measurement errors quoted in Tables 2–6 are $2\sigma_{mean}$ and precision on the Sm/Nd abundance ratios is about 0.01% relative deviation ($1\sigma$). Blanks measured during this work were 2 ng of Sr and 400 pg of Nd and Sm. Selected samples were analysed for the REE (La, Ce, Nd, Sm, Eu, Gd, Dy, Er, and Yb) by adapting the double cation exchange column techniques of CROCK et al. (1984), and mass spectrometry methods developed by SUN and NESBITT (1978). Within-run ratio relative standard deviations were less than 0.2%. Neodymium model parameters (depleted mantle $^{143}Nd/^{144}Nd$ 0.513108, $^{147}Sm/^{144}Nd$ 0.2157 and CHUR $^{143}Nd/^{144}Nd$ 0.512638, $^{147}Sm/^{144}Nd$ 0.1967) are based on those used by ALBARÈDE and BROUXEL (1987). A compilation of analyses on standards in this laboratory is presented in Table 1.

## GEOCHEMICAL AND ISOTOPIC RESULTS

Tables 2–7 present the major, trace, and rare earth element analyses and the isotopic data for the shales and basement rocks sampled. The ages quoted and used in the calculation of initial ratios were taken from or extrapolated from data given by WEBB et al. (1986), FANNING et al. (1988), or R. Flint (pers. commun.) for the Gawler Craton samples (Table 2) and summarized in PREISS (1987) for the Adelaidean sediments. The Kanmantoo samples were taken to lie between 526 Ma, the age of volcanics in the upper Normanville Group (COOPER et al., 1992), and 516 Ma, the age of the Delamerian Rathjen Gneiss (FODEN et al., 1992b). Isotopic, geochemical, and geochronological data for some representative Delamerian intrusive rocks are given in Table 5. An extensive geochemical and isotopic data base is now available for these rocks and additional data can be found in FODEN et al. (1990; 1993a,b), TURNER (1991), and TURNER et al., (1992a).

### Archaean Basement

Both mafic granulites and high-$SiO_2$ felsic gneisses were sampled from the Sleaford Complex on southern Eyre Pen-

insula (Fig. 1) along with two paragneisses and samples of unmetamorphosed rhyolite and basalt. In total, these samples define a range in initial $^{87}Sr/^{86}Sr$ of 0.6991–0.7143 with the more extreme samples possibly reflecting subsequent mobilization of Rb and Sr. $\epsilon$Nd values are more restricted, ranging from +4.2 to −6.2 (Fig. 7) with Nd depleted mantle model ages ($T_{DM}$) extending from 2.6 to 4.1 Ga. Rare earth patterns for the felsic gneisses and the paragneiss are LREE enriched and HREE depleted and the felsic gneiss has a negative Eu anomaly (Fig. 3). The mafic granulite, in contrast, has a flat REE pattern with higher HREE contents than the gneisses. The overall chemistry of these samples apparently differs from the well-described Lewisian Archaean of Scotland (WEAVER and TARNEY, 1981) in that the samples analysed here show an absence of positive Eu anomalies and no depletion of K, Rb, Th, and U.

### Early-Mid Proterozoic Basement

Early-Proterozoic rocks, covering a range of compositions from basaltic through to alkali granite, were sampled from the Hutchison Group and Lincoln Complex of Eyre Peninsula. Samples of the Cook Gap Schist and Broadview Schist were analyzed as potential crustal averages for the Early Proterozoic. With the exception of a basaltic dyke from Cape Donnington and the Broadview Schist ($\epsilon$Nd −7.4 and −7.5), these samples have moderately primitive Nd isotopic characteristics ($\epsilon$Nd 4.2 to −3.4; $T_{DM}$ 1.9–2.8) (Fig. 7). Initial $^{87}Sr/^{86}Sr$ values are highly variable and not correlated with $\epsilon$Nd, reflecting highly variable Rb/Sr ratios due to subsequent mobilization. The McGregor and Gawler Range Volcanics, the Corunna Conglomerate, and a shale from the Tarcoola Formation represent the Mid-Proterozoic with $\epsilon$Nd values ranging from +1.2 to −3.8 and $T_{DM}$ 2.0–2.3 Ga. Rare earth patterns for the Early- to Mid-Proterozoic samples (Fig. 4) show a remarkable consistency, considering the variations in lithology and bulk chemistry (see Table 3). They differ from the Archaean samples in that they lack HREE depletion and even the mafic samples are LREE-enriched. In absolute abundances and shape, these samples are very similar to those compiled by TAYLOR and MCLENNAN (1985) including their post-Archaean average shale (PAAS).

### Late Proterozoic Including Adelaidean

Emplacement of the Gairdner Dyke Swarm and eruption of the Wooltana Volcanics, and equivalents, preceded and accompanied the onset of Adelaidean sedimentation, respectively. A sample from the Gairdner Dyke Swarm has $\epsilon$Nd +2.9 and hydrothermally modified initial $^{87}Sr/^{86}Sr$ 0.7029 whilst one from the Wooltana Volcanics has $\epsilon$Nd +1.5 and initial $^{87}Sr/^{86}Sr$ 0.7153. A series of shales were sampled from the north central and southern Adelaide Fold Belt through the four principle subdivisions of the Adelaidean System: the Callanna Group, Burra Group, Umberatana Group, and Wilpena Group (Fig. 2). Variations in the bulk rock major and trace element chemistry largely reflect differences in their shale/sand ratio and with few exceptions (e.g., MgO, which declines throughout the Adelaidean sequence and was initially thought to represent a decaying volcanic contribution), there are no coherent trends. In general, the Adelaidean shows quite primitive $\epsilon$Nd with a trend, decreasing with age, from −4.4 to −10.8. The Callanna Group samples ($\epsilon$Nd −8.8 and −10.6) and the Appila Tillite from the Umberatana Group ($\epsilon$Nd −8.5) depart from this trend to more negative $\epsilon$Nd values (Fig. 7). Depleted mantle model ages lie between 1.8 and 2.2 Ga with a median of 1.9 Ga. With the exception of some of the older shales, initial $^{87}Sr/^{86}Sr$ is less variable than for the basement rocks, averaging around 0.7195. The rare earth patterns for the Adelaidean shales show a remarkable consistency of shape (average $La/Yb_N$ 10.6) and absolute abundance (Fig. 5), essentially indistinguishable from those for the Early- to Mid-Proteorozoic (Fig. 3).

The $\epsilon$Nd isotopic results on the four samples taken from the Bunyeroo Formation below the ejecta horizon are listed in Table 4 and, for the Sm-Nd system, show almost no variation of $\epsilon$Nd within error (~0.5 $\epsilon$ units). Neodymium model ages display more variation, extending from 1.9 to 2.2, though this is not correlated with sample location and most probably reflects the propagation of small errors in the $^{147}Sm/^{144}Nd$ ratio. Initial $^{87}Sr/^{86}Sr$ ranges from 0.7143 to 0.7342.

### Lower Palaeozoic

A stratigraphic succession of shales was taken through the Cambrian Normanville and Kanmantoo Groups from the southern Adelaide Fold Belt and Kangaroo Island. Despite the narrow time interval of their deposition (526 to 520–516 Ma), these samples display a considerable range of $\epsilon$Nd values (−9.4 to −13.4) which are, in general, more negative than those for the Adelaidean (Fig. 7; Table 5). Initial $^{87}Sr/^{86}Sr$ averages 0.7167, lower than that for the Adelaidean, whereas $T_{DM}$ show a similar range from 1.9 to 2.2 Ga but with a higher median of 2.1 Ga. In terms of their major and trace element chemistry, the Cambrian shales display less variation than those of the Adelaidean. This is reflected in the rare earth patterns for these Cambrian shales (Fig. 6) which show

Table 1. Compilation of analyses on standards, measurement errors are two sigma of the mean.

| *Standard* | *Rb ppm* | *Sr ppm* | *Nd ppm* | *Sm ppm* | *87Sr/86Sr* | *143Nd/144Nd* |
|---|---|---|---|---|---|---|
| BCR-1 | 46.43 | 322.1 | 28.63 | 6.54 | 0.704951 ±54 | 0.512507 ±24 |
| BHVO-1 | 9.24 | 396 | 25.08 | 6.17 | 0.703469 ±86 | 0.512964 ±05 |
| SRM 987 | | | | | 0.710183 ±37 | |
| La Jolla | | | | | | 0.511846 ±30 |

Table 2. Geochemical and isotopic analyses of Gawler Craton Archaean basement

| *Stratigraphy* | *Sleaford Complex* | *Sleaford Complex* | *Sleaford Complex* | *Sleaford Complex* | *Archaean* | *Archaean* | *Archaean Waddikee Rocks* | *Archaean* |
|---|---|---|---|---|---|---|---|---|
| *Sample #* | *JC3* | *446/256* | *446/F30* | *446/C142* | *DPA* | *DPB* | *6031RS60* | *6131RS14* |
| *Lithology* | *Leucogneiss* | *Augen gneiss* | *Basic granulite* | *Basic granulite* | *Rhyolite* | *Basalt* | *Paragneiss* | *Paragneiss* |
| *Locality* | *Cape Carnot* | *Cape Carnot* | *Cape Carnot* | *Cape Carnot* | *Devils playground* | *Devils playground* | *W Eyre Pen* | *Kimba* |
| *Est. Age (Ma)* | *2837* | *2643* | *2640* | *2640* | *2525* | *2525* | *2400* | *2400* |
| SiO2 | 76.75 | 70.08 | 47.54 | 50.69 | 73.15 | 58.13 | 73.24 | 65.16 |
| TiO2 | 0.25 | 0.64 | 2.67 | 0.84 | 0.33 | 1.36 | 0.27 | 0.84 |
| Al2O3 | 12.87 | 14.97 | 13.03 | 14.57 | 12.45 | 15.43 | 14.30 | 16.06 |
| Fe2O3 | 1.77 | 3.59 | 17.77 | 12.94 | 4.25 | 11.01 | 2.45 | 5.40 |
| MnO | 0.02 | 0.04 | 0.26 | 0.21 | 0.06 | 0.16 | 0.02 | 0.05 |
| MgO | 0.40 | 2.08 | 6.83 | 7.77 | 1.53 | 5.50 | 0.69 | 1.75 |
| CaO | 2.02 | 1.32 | 10.04 | 11.76 | 0.83 | 0.78 | 1.16 | 2.41 |
| Na2O | 3.75 | 2.79 | 1.64 | 0.94 | 3.69 | 4.01 | 3.24 | 3.32 |
| K2O | 2.31 | 5.50 | 0.25 | 0.65 | 1.66 | 0.49 | 4.62 | 4.46 |
| P2O5 | 0.03 | 0.09 | 1.09 | 0.06 | 0.05 | 0.26 | 0.09 | 0.22 |
| LOI | 0.33 | 0.15 | -0.54 | -0.01 | 2.31 | 3.58 | 0.27 | 0.48 |
| Total | 100.50 | 101.25 | 100.58 | 100.42 | 100.31 | 100.71 | 100.35 | 100.15 |
| Cr | 398 | 434 | 223 | 368 | 146 | 39 | 240 | 209 |
| Ni | 11 | 21 | 65 | 87 | 7 | 5 | 12 | 29 |
| Sc | 4 | 6 | 42 | 43 | 7 | 18 | 5 | 9 |
| V | 17 | 60 | 460 | 278 | 10 | 140 | 27 | 106 |
| Pb | 14.9 | 40 | 3 | 6.6 | 4.5 | 4.9 | 31 | 27 |
| Rb | 43.0 | 126.0 | 5.2 | 19.1 | 45.9 | 13.6 | 177.1 | 138.0 |
| Sr | 135.0 | 140.0 | 61.4 | 80.4 | 48.2 | 77.6 | 59.6 | 302.7 |
| Ba | 503 | 664 | 317 | 203 | 503 | 145 | 415 | 1331 |
| Ga | 13 | 19 | 20 | 17 | 15 | 18 | 17.6 | 21 |
| Nb | 6 | 7 | 17 | 4 | 12 | 7 | 12 | 13 |
| Zr | 171 | 275 | 170 | 51 | 300 | 166 | 135 | 196 |
| Y | 10 | 16 | 60 | 24 | 45 | 30 | 12 | 12 |
| Th | 11 | 52 | 1 | 1 | 11 | 4 | 32 | 18 |
| U | 0.2 | 2.3 | 0 | 0.7 | 1.8 | 0.6 | 14.4 | 0 |
| La | 39 | 88 | 37 | 7 | 28 | 23 | 28 | 52 |
| Ce | 70 | 215 | 70 | 17 | 59 | 36 | 61 | 130 |
| Nd | 17.12 | 40.24 | 28.80 | 8.34 | 26.46 | 28.56 | 29.37 | 32.62 |
| Sm | 2.64 | 6.78 | 7.49 | 2.32 | 6.09 | 5.93 | 5.46 | 6.59 |
| 87Sr/86Sr | 0.74320 ±3 | 0.79880 ±2 | 0.71321 ±1 | 0.73215 ±7 | 0.78548 ±7 | 0.72266 ±6 | 1.01260 ±4 | 0.74719 ±7 |
| 87Rb/86Sr | 0.9225 | 2.6066 | 0.1869 | 0.6711 | 2.7580 | 0.5076 | 8.6046 | 1.3209 |
| 87Sr/86Sr (t) | 0.70528 | 0.69912 | 0.70708 | 0.70651 | 0.68480 | 0.70414 | 0.71430 | 0.70140 |
| TSr (DM) | 3.2 | 2.6 | 4.9 | 3.2 | 2.1 | 2.9 | 2.5 | 2.4 |
| 143Nd/144Nd | 0.510916 ±28 | 0.510933 ±28 | 0.511981 ±26 | 0.511820 ±26 | 0.511528 ±36 | 0.511589 ±27 | 0.511377 ±20 | 0.511235 ±37 |
| 147Sm/144Nd | 0.0933 | 0.1019 | 0.1572 | 0.1679 | 0.1392 | 0.1255 | 0.1124 | 0.1221 |
| eNd (t) | 4.2 | -1.0 | 0.6 | -6.2 | -3.0 | 2.7 | -0.6 | -0.3 |
| TNd (DM) | 2.7 | 2.9 | 2.9 | 4.1 | 3.1 | 2.6 | 2.8 | 2.8 |

Samples JC3, 446/256, 446/F30 and 446/C142 from the collection of Fanning (1975).

even less variation than those for the Adelaidean shales. The average $La/Yb_N$ (13.9) is slightly higher than that for the Adelaidean, though overall both the Adelaidean and Cambrian shales have similar patterns, abundances, and small negative Eu anomalies.

Samples from the flysch-like turbidite sequences of the Lachlan Fold Belt spanning the upper Cambrian, the lower and upper Ordovician, and the Silurian have $\epsilon Nd$ (−8.8 to −11.1) similar to the shales from the Adelaide Fold Belt. The REE pattern, determined on the Bendigo shale shows greater LREE-enrichment than the Cambrian shales (Table 7, Fig. 6). Depleted mantle model ages are 1.8–1.9 Ga whilst initial $^{87}Sr/^{86}Sr$ for these samples (0.7132–0.7171) is slightly lower than the average for the Cambrian of the Adelaide Fold Belt.

### Glenelg River Complex and Antarctic Samples

Some preliminary data were collected on sediments from the Glenelg River Complex in western Victoria and the Wilson Terrane of North Victoria Land, Antarctica (Table 6). Three shales from the Glenelg River Complex have similar bulk rock and isotope chemistry (at 527 Ma: $\epsilon Nd$ −8.5 to −11.0; $T_{DM}$ 1.8–2 Ga; initial $^{87}Sr/^{86}Sr$ 0.7199 to 0.7261) whilst two Late Proterozoic samples from the Wilson terrane have (at 600 Ma) $\epsilon Nd$ −7.2 & −8.0, $T_{DM}$ 1.7 & 1.9 Ga and initial $^{87}Sr/^{86}Sr$ 0.7129 & 0.7142.

## INTERPRETATION AND DISCUSSION

The results previously given indicate that the Rb-Sr isotopic system has not remained undisturbed in the Archaean and some of the Early- and Mid-Proterozoic rocks and is not correlated with the Sm-Nd system. This is almost certain to be the case with the sediments due to the differential chemical behaviour of the Sm-Nd and Rb-Sr systems (e.g., GOLDSTEIN, 1988). Therefore, due to its greater robustness, much of the following discussion is restricted to the Sm-Nd isotopic sys-

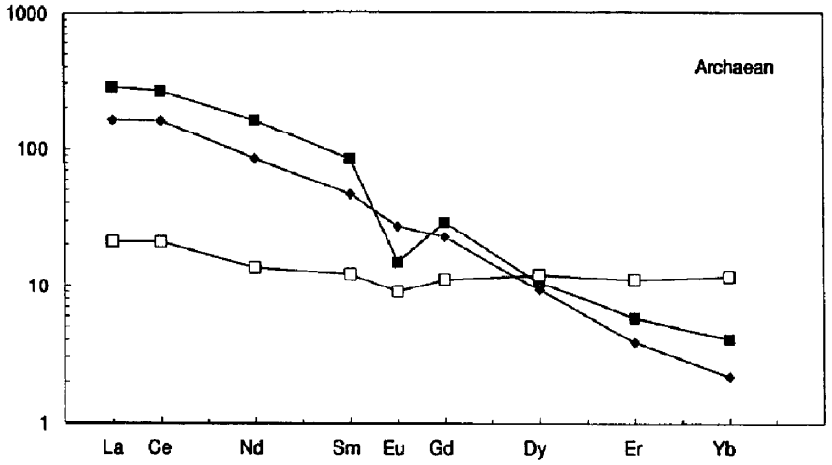


FIG. 3. Chondrite-normalized rare earth patterns for selected Archaean lithologies: mafic granulite (open squares); paragneiss (filled diamonds); augen gneiss (filled squares).

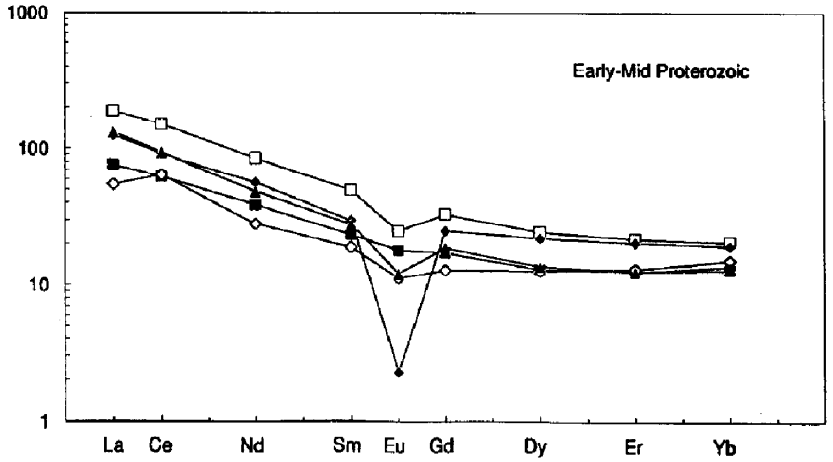


FIG. 4. Chondrite-normalized rare earth patterns for selected Early- and Mid-Proterozoic lithologies: Broadview Schist (open diamonds); basaltic dyke (filled squares); alkali granite (filled diamonds); Tarcoola Formation shale (filled triangles); ferro-hypersthene granite (open squares).

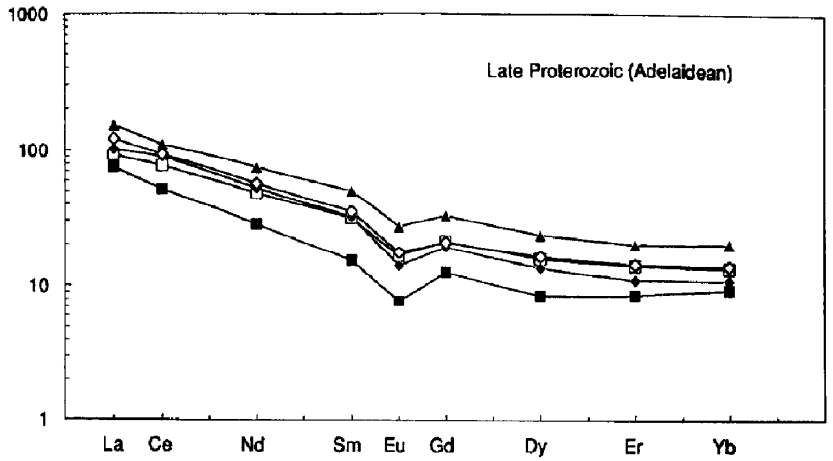


FIG. 5. Chondrite-normalized rare earth patterns for selected Adelaidean shales: Callanna Beds biotite schist (filled squares); Burra Group shale (open squares); Appila Tillite (filled diamonds); Etina Formation shale (open diamonds); Brachina Formation shale (filled triangles).

Table 3. Geochemical and isotopic analyses of Gawler Craton Early-Mid Proterozoic basement

| *Stratigraphy* | *Lincoln Complex* | *Lincoln Complex* | *Lincoln Complex* | *Lincoln Complex* | *Hutchinson Gp Cook Gap Schist* | *>Hutchinson Gp Broadview Schist* |
|---|---|---|---|---|---|---|
| *Sample #* | *515-B201* | *515-B26* | *515-B143* | *515-B152* | *939-90-13* | *6131RS147* |
| *Lithology* | *Gabbronorite* | *Basaltic dyke* | *Fe-hypersth Gt* | *Alkali granite* | *Schist* | *Schist* |
| *Locality* | *Donnington P.* | *Donnington P.* | *Donnington P.* | *Donnington P.* | *Lincoln* | *Lincoln* |
| *Est. Age (Ma)* | *1896* | *1850* | *1823* | *1820* | *1850* | *1800* |
| SiO2 | 55.96 | 52.89 | 65.37 | 77.01 | 61.85 | 61.89 |
| TiO2 | 0.80 | 0.80 | 0.87 | 0.07 | 0.69 | 0.85 |
| Al2O3 | 14.78 | 15.13 | 14.92 | 11.88 | 15.76 | 15.71 |
| Fe2O3 | 9.93 | 10.67 | 6.09 | 1.04 | 8.07 | 8.23 |
| MnO | 0.15 | 0.17 | 0.10 | 0.03 | 0.18 | 0.15 |
| MgO | 5.95 | 7.04 | 1.57 | 0.18 | 2.92 | 1.97 |
| CaO | 6.94 | 9.88 | 3.37 | 0.74 | 0.66 | 1.05 |
| Na2O | 2.47 | 2.47 | 2.98 | 3.03 | 1.82 | 3.68 |
| K2O | 2.21 | 1.13 | 4.43 | 5.20 | 4.72 | 4.50 |
| P2O5 | 0.20 | 0.19 | 0.24 | 0.00 | 0.13 | 0.18 |
| LOI | 0.44 | -0.10 | 0.09 | 0.22 | 2.42 | 2.08 |
| Total | 99.83 | 100.27 | 100.03 | 99.40 | 99.22 | 100.29 |
| Cr | 575 | 345 | 16 | 1 | 204 | 159 |
| Ni | 111 | 79 | 22 | 11 | 35 | 50 |
| Sc | 29 | 35 | 16 | 1 | 12 | 18 |
| V | 157 | 228 | 58 | 1 | 96 | 154 |
| Pb | 15 | 6.4 | 26.4 | 48.6 | 1101 | 5.8 |
| Rb | 102.0 | 28.0 | 201.0 | 413.0 | 229.2 | 181.1 |
| Sr | 231.0 | 318.0 | 171.0 | 12.0 | 69.4 | 109.0 |
| Ba | 500 | 728 | 885 | 6 | 542 | 1126 |
| Ga | 16 | 6.4 | 17.4 | 16 | 26 | 19 |
| Nb | 12 | 6 | 17 | 6 | 17 | 13 |
| Zr | 168 | 113 | 288 | 118 | 193 | 177 |
| Y | 31 | 26.1 | 47 | 52 | 36 | 21 |
| Th | 8 | 2.2 | 17 | 36 | 24 | 12 |
| U | 7.6 | 0.5 | 4.9 | 13.3 | 6.1 | 2.9 |
| La | 38 | 24 | 59 | 39 | 50 | 17 |
| Ce | 74 | 51 | 120 | 74 | 93 | 53 |
| Nd | 28.80 | 23.30 | 50.90 | 33.80 | 37.48 | 14.29 |
| Sm | 5.68 | 4.48 | 9.58 | 5.74 | 6.68 | 3.05 |
| 87Sr/86Sr | 0.73871 ±5 | 0.71087 ±3 | 0.79508 ±4 | 4.35480 ±4 | 0.94741 ±6 | 0.80340 ±6 |
| 87Rb/86Sr | 1.2789 | 0.2715 | 3.4043 | 99.4714 | 9.5653 | 4.8119 |
| 87Sr/86Sr (t) | 0.70381 | 0.70364 | 0.70580 | 1.75055 | 0.69280 | 0.67882 |
| TSr (DM) | 2.0 | 2.4 | 1.9 | 2.5 | 1.8 | 1.5 |
| 143Nd/144Nd | 0.511518 ±24 | 0.511284 ±13 | 0.511469 ±13 | 0.511728 ±16 | 0.511405 ±31 | 0.511456 ±47 |
| 147Sm/144Nd | 0.1194 | 0.1163 | 0.1139 | 0.1027 | 0.1077 | 0.1292 |
| eNd (t) | -3.0 | -7.4 | -3.4 | 4.2 | -2.9 | -7.5 |
| TNd (DM) | 2.5 | 2.8 | 2.4 | 1.9 | 2.4 | 2.9 |

Samples 515-B201, 515-B26, 515-B143 and 515-B152 from the collection of Mortimer (1984).

tem, in particular the $\epsilon$Nd evolution diagram in Fig. 7. Although it was attempted to restrict the sampling to shale-rich sediments, it is clear from the major element chemistry (Tables 2–6; Table 7) that some of the samples contain a significant sand component. However, a lack of correlation between $SiO_2$ and $\epsilon$Nd, or $T_{DM}$ and $^{147}Sm/^{144}Nd$ was noted, giving us confidence that the Sm-Nd isotopic systematics of these samples were not affected by sedimentary sorting in the manner observed by FROST and WINSTON (1987) or ZHAO et al. (1992). We concentrate our following discussion on $\epsilon$Nd values because the increased extrapolation beyond initial $\epsilon$Nd to derive $T_{DM}$ will magnify any errors in the $^{147}Sm/^{144}Nd$ ratio.

## Nature of the South Australian Archaean and Proterozoic Basement

The Archaean samples range of initial $\epsilon$Nd values are from +4.2 to −6.2 (Fig. 7). Five of the eight samples lie close to or above the bulk earth and depleted mantle curves indicating they may be largely mantle derived and that mantle derived magmatism was probably important during this period of Gawler Craton development. The remaining three samples have significantly negative $\epsilon$Nd, which indicates that they contain a major component of recycled older crustal material. The $^{147}Sm/^{144}Nd$ ratio, used to define a time trajectory line for each sample, results in a set of lines defining an envelope showing the time-evolution of these Archaean samples as a group. This envelope (Fig. 7) is then taken to represent the likely range of $\epsilon$Nd values for the Archaean basement at any particular time.

The range of $\epsilon$Nd values for the Early- to Mid-Proterozoic samples extends from similar to the depleted mantle $\epsilon$Nd to quite negative values for the Broadview Schist and a metabasaltic dyke. However, with the exception of these two later lithologies, all of the remaining lithologies plot outside and above the Archaean envelope at that time. This can be in-

Table 3. (*Continued*)

| *McGregor Volc* | *McGregor Volc* | *Pre-Adelaidean* | *Tarcoola Fm* | *GRV* | *Gairdner Dykes* |
|---|---|---|---|---|---|
| | | | | *Yardea* | |
| *MG2* | *MG4* | *939-90-11* | *939-90-14* | *884-Y10* | *RS27* |
| *Basalt* | *Rhyodacite* | *Conglomerate* | *Shale* | *Dacite* | *Dolerite* |
| *Corunna* | *Corunna* | *Corunna* | *Wilgena-1* | *Gawler Ranges* | *Stuart Shelf* |
| *1740* | *1740* | *1700* | *1654* | *1592* | *1000* |
| 47.44 | 65.59 | 68.71 | 72.50 | 68.02 | 50.55 |
| 1.06 | 0.77 | 0.45 | 0.40 | 0.67 | 1.57 |
| 14.57 | 14.82 | 15.33 | 12.24 | 13.68 | 12.44 |
| 11.78 | 5.29 | 3.28 | 4.18 | 5.10 | 13.53 |
| 0.21 | 0.13 | 0.03 | 0.04 | 0.14 | 0.31 |
| 8.63 | 1.56 | 1.48 | 1.64 | 0.57 | 7.95 |
| 12.12 | 2.17 | 0.19 | 0.61 | 2.03 | 10.99 |
| 2.30 | 2.56 | 1.06 | 0.99 | 3.29 | 1.77 |
| 0.84 | 5.57 | 5.38 | 3.37 | 5.19 | 0.18 |
| 0.29 | 0.23 | 0.05 | 0.08 | 0.17 | 0.10 |
| 0.51 | 0.70 | 3.16 | 4.33 | 0.95 | 0.48 |
| 99.75 | 99.39 | 99.12 | 100.38 | 99.81 | 99.87 |
| 657 | 13 | 22 | 88 | 5 | 216 |
| 262 | 7 | 12 | 20 | 3 | 89 |
| 33 | 15 | 8 | 7 | 15 | 44 |
| 225 | 53 | 35 | 41 | 20 | 356 |
| 8 | 17 | 35 | 16 | 26 | |
| 53.7 | 238.2 | 235.0 | 161.7 | 208.4 | 6.7 |
| 662.0 | 218.0 | 70.4 | 36.1 | 165.6 | 154.6 |
| 183 | 887 | 846 | 585 | 1410 | 27 |
| 16 | 19 | 16 | 15 | 21 | 22 |
| 13 | 16 | 15 | 13 | 21 | 5.1 |
| 91 | 305 | 210 | 144 | 432 | 87 |
| 24 | 43 | 35 | 29 | 66 | 28 |
| 4.7 | 20.3 | 13 | 16 | 31 | |
| | 4.5 | 4.3 | 2.7 | 8.5 | |
| 39 | 67 | 45 | 41 | 84 | 6 |
| 75 | 134 | 89 | 76 | 178 | 18 |
| 33.46 | 55.53 | 37.00 | 26.67 | 68.52 | 10.70 |
| 5.15 | 9.83 | 6.87 | 4.94 | 13.07 | 3.29 |
| 0.71011 ±9 | 0.78493 ±3 | 0.92249 ±4 | 0.99480 ±9 | 0.78767 ±9 | 0.70479 ±5 |
| 2.3495 | 3.1619 | 9.6606 | 12.9818 | 3.6441 | 0.1257 |
| 0.65133 | 0.70584 | 0.68644 | 0.68629 | 0.70435 | 0.70299 |
| 0.2 | 1.8 | 1.6 | 1.6 | 1.6 | 1.4 |
| 0.511418 ±16 | 0.511440 ±31 | 0.511755 ±18 | 0.511679 ±20 | 0.511593 ±33 | 0.512714 ±25 |
| 0.0926 | 0.1070 | 0.1124 | 0.1121 | 0.1154 | 0.1860 |
| -0.6 | -3.4 | 1.2 | -0.8 | -3.8 | 2.9 |
| 2.1 | 2.3 | 2.0 | 2.1 | 2.3 | 2.0 |

terpreted in two ways: either there exists more isotopically primitive Archaean rocks from which the Early- to Mid-Proterozoic ones were derived, or alternatively, most of these rocks contain both a recycled Archaean and a mantle component. If the latter hypothesis is correct, then the Early- to Mid-Proterozoic development of the Gawler Craton also involved significant mantle input. Support for this lies in the existence of both mafic intrusives and volcanics within this stratigraphy. An envelope describing the evolution of the Early- to Mid-Proterozoic samples is defined in Fig. 7 and, due to the generally lower $^{147}Sm/^{143}Nd$ of these samples, this envelope intersects and largely overlaps the Archaean one after the Late Proterozoic.

Basement areas also outcrop to the northeast of the Adelaide Fold Belt at Mt. Painter and Broken Hill, and in addition there are inliers within the fold belt itself. However, the limited published data on these rocks (MCCULLOCH, 1987) indicate they are broadly similar to the Gawler Craton analyses presented here.

## Origin of the Adelaidean

If the Adelaidean sediments were simply derived by erosion of Gawler Craton material, they would be expected to lie within the $\epsilon Nd$ range defined by the Archaean and Early- to Mid-Proterozoic envelopes; but inspection of Fig. 7 shows this is not the case. The majority of the shales have higher $\epsilon Nd$ lying above the basement envelopes, though two samples from the Callanna Group and the Sturtian Tillite have more negative $\epsilon Nd$ and do lie within the basement envelopes (Fig. 7). Figure 8a shows this in detail and also shows that a similar pattern is observed for the $T_{DM}$ ages which are highest for the Callanna samples (2.2–2.1 Ga) but rapidly drop in the Burra Group (~1.8 Ga), and then rise from 1.8 to 2.2 Ga through the remaining Adelaidean sequence with the Sturtian Tillite again forming an anomaly. Notably these model ages are generally younger than those for the basement (see Table 4).

Table 4. Geochemical and isotopic analyses of Adelaidean shales and synchronous mafic volcanics

| *Stratigraphy* | *Wooltana Volc* | *Willouran Callana Beds* | *Willouran Callana Beds* | *Torrensian Burra Group* | *Torrensian Belair sub-Gp* | *Sturtian Appila Tillite* | *Sturtian Tapley Hill Fm* | *Marinoan Umberatana* |
|---|---|---|---|---|---|---|---|---|
| *Sample #* | *W6* | *939-90-9* | *939-90-8* | *939-90-7* | *90-Bel-1* | *814-041-53* | *939-90-10* | *819-18* |
| *Lithology* | *Basalt* | *Shale* | *Bt schist* | *shale* | *shale* | *tillite* | *shale* | *shale* |
| *Locality* | *E Flinders* | *Blinman Diapir* | *Arkaroola* | *Clarendon* | *Belair* | *Sturt George* | *Tapley Hill* | *Etina Fm Flinders Ra.* |
| *Est. Age (Ma)* | *900* | *850* | *850* | *840* | *820* | *800* | *750* | *700* |
| SiO2 | 50.49 | 49.38 | 49.96 | 64.94 | 65.08 | 69.88 | 55.64 | 56.37 |
| TiO2 | 1.77 | 0.49 | 0.92 | 0.84 | 1.25 | 0.75 | 0.90 | 0.78 |
| Al2O3 | 13.81 | 10.65 | 18.98 | 14.84 | 14.77 | 10.99 | 13.26 | 13.35 |
| Fe2O3 | 12.67 | 3.83 | 4.67 | 7.61 | 6.35 | 4.92 | 6.33 | 6.14 |
| MnO | 0.25 | 0.05 | 0.02 | 0.01 | 0.02 | 0.00 | 0.06 | 0.08 |
| MgO | 8.16 | 12.52 | 12.20 | 3.55 | 3.04 | 4.39 | 6.71 | 3.93 |
| CaO | 4.25 | 6.02 | 0.12 | 0.36 | 0.12 | 1.01 | 3.82 | 6.03 |
| Na2O | 4.38 | 0.39 | 0.68 | 1.16 | 1.14 | 0.26 | 1.61 | 1.54 |
| K2O | 0.63 | 3.61 | 8.77 | 3.21 | 4.06 | 3.12 | 2.85 | 2.93 |
| P2O5 | 0.14 | 0.10 | 0.07 | 0.18 | 0.11 | 0.11 | 0.19 | 0.16 |
| LOI | 2.82 | 12.63 | 2.11 | 4.12 | 3.62 | 4.39 | 8.33 | 8.51 |
| Total | 99.37 | 99.67 | 98.50 | 100.82 | 99.56 | 99.82 | 99.70 | 99.82 |
| Cr | 203 | 60 | 136 | 121 | | 72 | 97 | 99 |
| Ni | 114 | 29 | 48 | 63 | 26 | 14 | 44 | 35 |
| Sc | 47 | 11 | 21 | 14 | 16 | 12 | 15 | 16 |
| V | 297 | 73 | 168 | 215 | 135 | 91 | 186 | 137 |
| Pb | | 3.9 | 0 | 31 | 12 | 11.2 | 29 | 20 |
| Rb | 25.0 | 66.2 | 336.4 | 145.8 | 186.5 | 119.7 | 114.4 | 122.4 |
| Sr | 141.9 | 38.4 | 43.3 | 36.3 | 76.8 | 25.3 | 179.6 | 105.7 |
| Ba | 79 | 289 | 1020 | 651 | 360 | 321 | 481 | 384 |
| Ga | 21 | 11 | 23 | 18 | 19 | 12 | 16 | 16 |
| Nb | 6 | 10 | 17 | 12 | 16 | 13 | 13 | 13 |
| Zr | 105 | 128 | 161 | 151 | 235 | 280 | 173 | 181 |
| Y | 28 | 18 | 32 | 31 | 38 | 26 | 29 | 30 |
| Th | | 7 | 8 | 8 | 18 | 11 | 8.8 | 10 |
| U | | 3.1 | 2 | 3.3 | 3.6 | 3 | 4.4 | 3 |
| La | 9 | 19 | 23 | 29 | 42 | 32 | 40 | 38 |
| Ce | 24 | 38 | 42 | 62 | 83 | 73 | 73 | 76 |
| Nd | 15.60 | 16.89 | 8.62 | 29.62 | 39.57 | 26.11 | 32.66 | 29.76 |
| Sm | 4.33 | 3.27 | 1.63 | 6.15 | 7.86 | 5.27 | 6.56 | 5.95 |
| 87Sr/86Sr | 0.72189 ±5 | 0.77728 ±5 | 0.84297 ±5 | 0.81517 ±5 | 0.77533 ±7 | 0.85421 ±5 | 0.73879 ±6 | 0.74678 ±4 |
| 87Rb/86Sr | 0.5099 | 4.9933 | 22.5259 | 11.6381 | 7.3211 | 13.7161 | 1.8451 | 3.3530 |
| 87Sr/86Sr (t) | 0.71533 | 0.71665 | 0.56947 | 0.67552 | 0.68958 | 0.69751 | 0.71904 | 0.71329 |
| TSr (DM) | 2.8 | 1.1 | 0.4 | 0.7 | 0.7 | 0.8 | 1.4 | 0.9 |
| 143Nd/144Nd | 0.512544 ±28 | 0.511744 ±22 | 0.511639 ±27 | 0.512024 ±17 | 0.511947 ±24 | 0.511811 ±23 | 0.512005 ±18 | 0.511962 ±30 |
| 147Sm/144Nd | 0.1679 | 0.1172 | 0.1146 | 0.1257 | 0.1202 | 0.1222 | 0.1214 | 0.1210 |
| eNd (t) | 1.5 | -8.8 | -10.6 | -4.4 | -5.5 | -8.5 | -5.1 | -6.4 |
| TNd (DM) | 1.8 | 2.1 | 2.2 | 1.8 | 1.9 | 2.1 | 1.8 | 1.8 |

JENKINS (1990) inferred a multiple sequence of rift- and thermal-sag-phases for the Adelaide Fold Belt. This is not revealed by the present data (possibly due to the large sampling intervals), which is interpreted in terms of one major cycle (Fig. 8a). The earliest sediments, the Callanna Group, are likely to have been deposited in restricted, early intracratonic rifts during the rift-phase of sedimentation and therefore their $\epsilon$Nd signature reflects the local basement material now exposed on the Gawler Craton and inliers in the fold belt. The remaining Adelaidean sediments are areally extensive and belong to the thermal-sag-phase of sedimentation (Fig. 8a). Their higher $\epsilon$Nd indicates that enlargement of the source area allowed sampling of isotopically more primitive source materials. A more extensive provenance region for these sag-phase sediments is also supported by the $\epsilon$Nd homogeneity of the four Bunyeroo samples. This is quite remarkable considering the lateral distance over which the samples were taken ($\sim$1000 km) and indicates a very large and quite distal provenance region in order to allow blending of differing source detritus. Importantly, this result suggests that sedimentary packages can be quite uniform along strike so that the variations described in this paper are likely to represent true stratigraphic changes rather than along-strike variations in provenance contributions. Continued excavation of the provenance region then causes the trend of gradual decrease in $\epsilon$Nd and increase in model age, presumably as progressively older and more evolved basement materials are eroded. In addition, stratigraphic overturn, whereby Callanna Group material was brought to the surface in diapirs and recombined in the later Umberatana and Wilpena Group sediments (N. Lemon, pers. commun.) would contribute to the lowering of $\epsilon$Nd and increase in model age in these later sediment signatures.

As Fig. 7 shows, the sag-phase sediments do not have $\epsilon$Nd signatures like the Gawler Craton basement material. This is intriguing and several possibilities arise. These sediments

Table 4. (*Continued*)

| *Marinoan* *Umberatana* *819-24* *shale* *Enorama* *Flinders Ra.* *680* | *Marinoan* *Wilpena* *939-90-6* *shale* *Flinders Ra.* *650* | *Marinoan* *Brachina Fm* *819-84* *shale* *Flinders Ra.* *600* | *Marinoan* *Brachina Fm* *474-K* *shale* *Echunga* *600* | *Marinoan* *Bunyeroo Fm* *939-90-13* *shale* *Officer Basin* *600* | *Marinoan* *Bunyeroo Fm* *939-90-14* *shale* *Pichi Richi* *600* | *Marinoan* *Bunyeroo Fm* *939-90-15* *shale* *Lake Torrens* *600* | *Marinoan* *Bunyeroo Fm* *939-90-16* *shale* *Mena Mena* *600* |
|---|---|---|---|---|---|---|---|
| 55.95 | 60.16 | 68.42 | 59.51 | 60.08 | 76.38 | 57.07 | 59.61 |
| 0.81 | 1.53 | 1.24 | 0.76 | 0.86 | 0.85 | 0.83 | 0.86 |
| 12.42 | 18.25 | 13.11 | 15.55 | 15.66 | 11.72 | 14.61 | 15.40 |
| 5.85 | 7.41 | 6.95 | 6.93 | 8.25 | 2.33 | 7.81 | 11.48 |
| 0.11 | 0.03 | 0.05 | 0.16 | 0.08 | 0.06 | 0.20 | 0.47 |
| 4.15 | 2.64 | 2.22 | 5.14 | 3.43 | 0.37 | 3.93 | 2.50 |
| 7.02 | 0.25 | 0.43 | 2.86 | 0.63 | 0.37 | 2.91 | 0.35 |
| 1.62 | 2.28 | 3.05 | 1.68 | 1.83 | 4.19 | 1.71 | 0.41 |
| 2.72 | 4.88 | 1.23 | 5.30 | 4.97 | 2.20 | 4.15 | 4.84 |
| 0.16 | 0.18 | 0.24 | 0.19 | 0.15 | 0.12 | 0.13 | 0.15 |
| 8.91 | 3.98 | 2.63 | 1.02 | 4.00 | 1.29 | 6.62 | 3.76 |
| 99.72 | 101.59 | 99.57 | 99.10 | 99.94 | 99.88 | 99.97 | 99.83 |
| 96 | 149 | 57 | 292 | 106 | 63 | 88 | 89 |
| 36 | 39 | 31 | 49 | 48 | 22 | 46 | 54 |
| 15 | 19 | 11 | 14 | 18 | 8 | 18 | 17 |
| 128 | 197 | 110 | 113 | 132 | 132 | 112 | 108 |
| 19 | 27 | 48 | 5.4 | 19 | 8 | 53 | 11 |
| 114.6 | 221.1 | 56.4 | 241.2 | 192.2 | 77.4 | 186.8 | 220.1 |
| 113.8 | 39.3 | 55.0 | 118.4 | 90.7 | 80.3 | 78.6 | 53.4 |
| 498 | 410 | 236 | 1786 | 445 | 515 | 416 | 408 |
| 15 | 24 | 14 | 18 | 23 | 12 | 20 | 21 |
| 13 | 23 | 15 | 13 | 15 | 15 | 16 | 17 |
| 195 | 273 | 305 | 176 | 164 | 303 | 175 | 171 |
| 29 | 47 | 36 | 20 | 31 | 44 | 30 | 27 |
| 7.8 | 19 | 8.6 | 13 | 21 | 21 | 23 | 22 |
| 4.3 | 6.7 | 3.1 | 2.3 | 1.9 | 3 | 3.5 | 3.4 |
| 33 | 61 | 48 | 74 | 47 | 35 | 45 | 41 |
| 65 | 115 | 90 | 109 | 89 | 86 | 87 | 79 |
| 29.11 | 48.61 | 29.93 | 44.34 | 38.27 | 54.67 | 35.67 | 36.25 |
| 5.88 | 9.44 | 6.94 | 7.55 | 7.27 | 11.25 | 6.81 | 6.75 |
| 0.74166 ±3 | 0.86179 ±6 | 0.74394 ±3 | 0.76928 ±3 | 0.78669 ±6 | 0.75185 ±42 | 0.78633 ±5 | 0.81635 ±8 |
| 2.9172 | 16.2836 | 2.9706 | 5.9031 | 6.1362 | 2.7940 | 6.8858 | 11.9275 |
| 0.71335 | 0.71080 | 0.71852 | 0.71877 | 0.73419 | 0.72795 | 0.72742 | 0.71430 |
| 0.9 | 0.7 | 1.0 | 0.8 | 1.0 | 1.2 | 0.9 | 0.7 |
| 0.511934 ±23 | 0.511902 ±31 | 0.512092 ±16 | 0.511738 ±39 | 0.51181 ±16 | 0.511803 ±22 | 0.511818 ±15 | 0.511792 ±20 |
| 0.1222 | 0.1175 | 0.1404 | 0.1030 | 0.1149 | 0.1245 | 0.1155 | 0.1126 |
| -7.3 | -7.8 | -6.3 | -10.4 | -9.9 | -10.8 | -9.8 | -10.1 |
| 1.9 | 1.9 | 2.1 | 1.9 | 2.0 | 2.2 | 2.0 | 1.9 |

could, perhaps, have been derived from a more primitive, unrecognised source terrane, possibly lying to the east or south of the present Adelaidean outcrop or represent mixtures of such a terrane with the more evolved Gawler Craton material. A complete switch from one source terrane to another is not supported by the present chemical data. For example, no obvious distinction (or correlation) was found, between the rift-phase and sag-phase sediments on plots of Zr/Nb vs. $\epsilon$Nd. Alternatively, the sediments may represent mixtures of Gawler Craton material with detritus from mantle derived volcanic material. The Wooltana Basalts most probably did contribute to the sedimentary detritus; however, simple mixing calculations require addition of 40–50% Wooltana detritus to Callana-type sediment to achieve the Nd isotopic composition of the sag-phase sediments. It seems improbable that this volume of contribution could have continued over the entire ~200 Ma thermal-sag-phase sequence which does not show systematically higher Cr or Ni contents that might be predicted from a major basaltic contribution. Furthermore, volcanics are generally absent after the Wooltana episode which occurred during the inception of the Adelaidean system and the highest $\epsilon$Nd values are seen in the Burra Group not in the Callanna Group. Therefore, if the contribution of such volcanic detritus was important its influence was delayed until basin formation advanced and the provenance area enlarged. In our preferred model, outlined previously, the signature resulted from the expansion of the provenance area allowing access of, and blending with, more primitive materials than those currently exposed on the Gawler Craton. For example, the Gairdner Dyke Swarm may represent the feeder zone to a flood basalt province that was eroded and mixed with Gawler Craton detritus to produce the isotopic signature of the Adelaidean sag-phase sediments. In either case, a contribution from isotopically primitive material is required.

Of particular interest is the departure of the Appila Tillite, from the isotopic trend just described (see Fig. 8a), to rift-

Table 5. Geochemical and isotopic analyses of Normanville and Kanmantoo Group shales, synchronous mafic volcanics and Delamerian magmatic rocks

| *Stratigraphy* | *Normanville* | *Truro Volc* | *Tunkillo* | *Normanville* | *Kanmantoo* | *Kanmantoo* | *Kanmantoo* | *Kanmantoo* | *Kanmantoo* |
|---|---|---|---|---|---|---|---|---|---|
| | *Sellick Hill* | | | *Heatherdale* | *Carrickalinga* | *Carrickalinga* | *Backstairs Pa.* | *Tapanappa* | *Tunkalilla* |
| *Sample #* | *939-90-5* | *876-1013* | *AH-1* | *90-Car-1* | *876-1017* | *876-1018* | *474-318* | *474-K40* | *474-354* |
| *Lithology* | *shale* | *Basalt* | *Amphibolite* | *shale* | *shale* | *shale* | *shale* | *shale* | *shale* |
| *Locality* | *Sellicks Hill* | *Dutton* | *Tunkillo* | *Carrickalinga* | *Carrickalinga* | *Carrickalinga* | *Monarto* | *Kangaroo Is.* | *Victor Harbor* |
| *Est. Age (Ma)* | *526* | *526* | *525* | *525* | *523* | *522* | *521* | *520* | *519* |
| SiO2 | 70.22 | 42.37 | 47.83 | 42.15 | 65.13 | 61.87 | 60.05 | 61.00 | 60.14 |
| TiO2 | 0.75 | 2.48 | 1.87 | 0.51 | 0.76 | 0.86 | 0.73 | 0.64 | 0.75 |
| Al2O3 | 14.15 | 12.90 | 13.97 | 10.31 | 15.45 | 16.38 | 18.63 | 15.67 | 18.46 |
| Fe2O3 | 4.16 | 11.56 | 13.25 | 3.32 | 6.46 | 7.86 | 9.96 | 4.44 | 7.17 |
| MnO | 0.00 | 0.20 | 0.29 | 0.04 | 0.08 | 0.07 | 0.11 | 0.13 | 0.06 |
| MgO | 1.58 | 12.47 | 6.55 | 2.53 | 3.00 | 3.33 | 3.74 | 2.24 | 3.27 |
| CaO | 0.29 | 11.12 | 12.10 | 19.32 | 0.58 | 0.36 | 0.28 | 8.91 | 0.19 |
| Na2O | 1.62 | 1.43 | 2.84 | 0.88 | 2.46 | 1.99 | 1.71 | 0.51 | 1.50 |
| K2O | 3.20 | 0.84 | 1.05 | 2.83 | 3.17 | 3.65 | 3.08 | 2.61 | 3.85 |
| P2O5 | 0.19 | 0.85 | 0.21 | 0.34 | 0.16 | 0.14 | 0.17 | 0.16 | 0.08 |
| LOI | 3 42 | 3.29 | 0.23 | 17.54 | 2.81 | 3.72 | 1.70 | 3.07 | 4.24 |
| Total | 99.58 | 99.51 | 100.19 | 99.77 | 100.06 | 100.23 | 100.16 | 99.38 | 99.71 |
| Cr | 98 | 581 | 179 | | 154 | 148 | 405 | 247 | 149 |
| Ni | 40 | 274 | 46 | 29 | 44 | 57 | 60 | 23 | 48 |
| Sc | 11 | 32 | 42 | 13 | 13 | 14 | 16 | 15 | 15 |
| V | 126 | 247 | 371 | 73 | 108 | 126 | 133 | 99 | 125 |
| Pb | 11 | 5 | 6.3 | 13 | 23 | 31 | 0 | 23 | 21 |
| Rb | 150.2 | 17.0 | 29.0 | 113.6 | 146.0 | 177.5 | 144.1 | 155.0 | 185.5 |
| Sr | 178.3 | 780.4 | 183.0 | 274.3 | 158.3 | 105.7 | 52.7 | 577.9 | 115.6 |
| Ba | 2356 | 573 | 100 | 605 | 704 | 718 | 800 | 292 | 683 |
| Ga | 16 | 16 | 21 | 14 | 20 | 21 | 23 | 17 | 23 |
| Nb | 15 | 89 | 10.8 | 11 | 15 | 18 | 15 | 13 | 15 |
| Zr | 196 | 250 | 124 | 90 | 141 | 118 | 144 | 157 | 138 |
| Y | 40 | 28 | 39 | 14 | 28 | 24 | 49 | 28 | 39 |
| Th | 16 | 5.8 | 2 | 14 | 9.1 | 7 | 13 | 15 | 14 |
| U | 5 | 1.4 | 0.2 | 4 | 3.5 | 4.1 | 5.9 | 3.6 | 5.3 |
| La | 53 | 112 | 9 | 27 | 36 | 34 | 43 | 42 | 82 |
| Ce | 112 | 179 | 24 | 48 | 74 | 68 | 76 | 89 | 79 |
| Nd | 38.40 | 75.16 | 17.07 | 17.34 | 32.39 | 29.28 | 39.42 | 35.42 | 37.95 |
| Sm | 7.68 | 12.36 | 5.10 | 3.40 | 6.38 | 5.81 | 7.38 | 6.77 | 6.63 |
| 87Sr/86Sr | 0.73167 ±5 | 0.70369 ±2 | 0.71134 ±8 | 0.72009 ±6 | 0.73632 ±5 | 0.75344 ±9 | 0.77864 ±5 | 0.71619 ±8 | 0.75153 ±7 |
| 87Rb/86Sr | 2.4403 | 0.0632 | 0.4432 | 1.1711 | 2.6704 | 4.8646 | 7.9226 | 0.7770 | 4.6483 |
| 87Sr/86Sr (t) | 0.71338 | 0.70320 | 0.70802 | 0.71133 | 0.71641 | 0.71725 | 0.71981 | 0.71041 | 0.71714 |
| TSr (DM) | 0.8 | 2.2 | 1.4 | 1.1 | 0.9 | 0.7 | 0.7 | 1.2 | 0.7 |
| 143Nd/144Nd | ).511802 ±28 | ).512560 ±21 | 0.512677 ±25 | 0.511824 ±28 | 0.511482 ±29 | 0.511894 ±27 | 0.511704 ±44 | 0.511711 ±20 | 0.511679 ±29 |
| 147Sm/144Nd | 0.1209 | 0.0995 | 0.1807 | 0.1186 | 0.1191 | 0.1200 | 0.1132 | 0.1156 | 0.1057 |
| eNd (t) | -11.2 | 5.0 | 1.8 | -10.7 | -10.4 | -9.4 | -12.7 | -12.7 | -12.7 |
| TNd (DM) | 2.1 | 0.7 | 1.9 | 2.0 | 2.0 | 1.9 | 2.1 | 2.1 | 2.0 |

phase $\epsilon$Nd and $T_{DM}$ values like those of the Callanna Group. The Sturtian glaciogenic sediments (which include the Appila Tillite) contain gneissic basement dropstones (YOUNG and GOSTIN, 1988) and are interpreted as a transitory restriction of the source region to the local basement material again. Uplift of rift-shoulders that lead to glaciation would simultaneously bar sedimentary detritus from the broader provenance region beyond the rift-shoulders. Such an interpretation implies renewed or increased extension during early Umberatana time consistent with evidence for syn-depositional normal faulting (COATS, 1981). Subsequent recovery is demonstrated by the return to the sag-phase isotopic pattern illustrated by the isotopic composition of the overlying Tapley Hill Formation (Fig. 8a).

## Origin of the Cambrian (Normanville and Kanmantoo) Sequences

The Cambrian sediments do not appear to form a continuation of the Adelaidean isotopic pattern in any simple way (Fig. 7); they have, on average, slightly older model ages than the Adelaidean (Fig. 8b) but their $\epsilon$Nd values are distinctly lower (Figs. 7 and 8b). Weathering and sedimentary recycling (e.g., NESBITT et al., 1990; ZHAO et al., 1992) can result in LREE-enrichment, and such a process might be invoked to explain the higher average $La/Yb_N$ of the Cambrian sediments, relative to the Adelaidean. However, LREE-enrichment (i.e., lower Sm/Nd) will result in calculated $\epsilon$Nd and $T_{DM}$ values that are higher and lower, respectively, and since the opposite is observed the data would seem to preclude these Cambrian sediments being entirely derived as reworked Adelaidean material.

A change in provenance region or relative source contributions is clearly required between the Adelaidean and Cambrian sequences. This corresponds broadly with the change from shelf to deep water depositional environment which occurred, specifically, at the base of the Kanmantoo Group. One scenario is that this change involved distancing or expiry of a relatively primitive terrane important in the provenance of the Adelaidean sediments, leaving the more evolved Gawler

Table 5. (*Continued*)

| *Kanmantoo* *Balquhidder* *474-288* *shale* *Torrens Vale* | *Kanmantoo* *Petrel Cove* *474-CN1* *shale* *Port Elliot* | *Kanmantoo* *Boxing Bay* *939-BB-1* *conglom/shale* *Kangaroo Is* | *Kanmantoo* *Boxing Bay* *939-BB-3* *conglom/shale* *Kangaroo Is* | *Delamerian* *I-type* *89-R1* *Rathjen Gneiss* *Hills* | *Delamerian* *S-type* *KI 89-5* *granite* *Kangaroo Is* | *Delamerian* *I-type* *779-52* *granodiorite* *Reedy Creek* | *Delamerian* *A-type* *861-93* *granite* *Mannum* | *Delamerian* *Mafic* *898-350* *gabbro* *Mt Pleasant* |
|---|---|---|---|---|---|---|---|---|
| *518* | *517* | *516* | *516* | *516* | *512* | *490* | *487* | *487* |
| 62.34 | 55.02 | 59.87 | 46.86 | 73.97 | 71.50 | 65.60 | 72.24 | 49.00 |
| 0.77 | 0.80 | 0.75 | 0.62 | 0.44 | 0.46 | 0.67 | 0.38 | 0.88 |
| 16.71 | 19.93 | 15.81 | 13.00 | 12.45 | 13.31 | 16.20 | 13.77 | 20.89 |
| 6.66 | 8.02 | 9.00 | 5.93 | 2.81 | 3.71 | 4.57 | 2.13 | 7.79 |
| 0.11 | 0.10 | 0.04 | 0.09 | 0.03 | 0.06 | 0.06 | 0.07 | 0.14 |
| 3.27 | 4.25 | 3.75 | 3.57 | 0.81 | 1.67 | 1.77 | 0.55 | 5.63 |
| 2.63 | 1.91 | 0.29 | 10.37 | 1.66 | 1.84 | 3.38 | 0.87 | 13.14 |
| 2.82 | 1.78 | 1.53 | 0.87 | 3.55 | 2.59 | 4.36 | 4.01 | 2.38 |
| 3.17 | 5.31 | 4.58 | 4.95 | 3.17 | 3.48 | 2.00 | 5.66 | 0.17 |
| 0.18 | 0.15 | 0.16 | 0.30 | 0.10 | 0.07 | 0.24 | 0.08 | 0.07 |
| 0.97 | 1.85 | 3.84 | 12.44 | 0.25 | 0.54 | 1.20 | 0.36 | 0.18 |
| 99.63 | 99.12 | 99.62 | 99.00 | 99.24 | 99.23 | 100.05 | 100.12 | 100.27 |
| 189 | 192 | 207 | 147 | 17 | 68 | 17 | 5 | 155 |
| 48 | 59 | 50 | 38 | 7 | 25 | 19 | 1 | 63 |
| 16 | 20 | 13 | 16 | 8.7 | 12 | 10 | 5.5 | 29 |
| 114 | 150 | 106 | 92 | 40 | 67 | 81 | 21 | 208 |
| 19 | 16 | 13 | 49 | 5 | | 8 | 12 | 2 |
| 158.4 | 212.6 | 249.1 | 176.0 | 137.2 | 152.2 | 92.0 | 189.8 | 7.6 |
| 210.5 | 138.0 | 69.8 | 112.8 | 110.3 | 151.9 | 518.0 | 133.3 | 136.7 |
| 572 | 1471 | 519 | 420 | 697 | 596 | 857 | 641 | 33 |
| 19 | 27 | 25 | 19 | 16 | | 19 | 21 | 17 |
| 15 | 17 | 16 | 13 | 12.8 | 13 | 13 | 49 | 2 |
| 164 | 117 | 162 | 135 | 260 | 175 | 143 | 334 | 47 |
| 32 | 35 | 22 | 29 | 41 | 53 | 6 | 62 | 19 |
| 13 | 15 | 19 | 18 | 25 | | 3 | 27 | 0.9 |
| 4.1 | 4.8 | 5 | 5 | 4.6 | | 4.3 | 9.4 | 1 |
| 58 | 37 | 63 | 41 | 48 | 27 | 15 | 80 | 3 |
| 103 | 74 | 99 | 74 | 102 | 67 | 26 | 155 | 8 |
| 38.15 | 31.01 | 34.40 | 27.42 | 56.89 | 17.43 | 10.81 | 59.89 | 5.77 |
| 7.34 | 5.89 | 5.76 | 5.24 | 10.99 | 3.64 | 1.98 | 10.53 | 1.88 |
| 0.73925 ±5 | 0.72588 ±3 | 0.78982 ±8 | 0.75038 ±5 | 0.73701 ±5 | 0.73999 ±5 | 0.70964 ±9 | 0.73377 ±2 | 0.70453 ±4 |
| 2.1797 | 4.4618 | 10.3395 | 4.5292 | 3.4714 | 2.8906 | 0.5144 | 4.1256 | 0.1611 |
| 0.72315 | 0.72001 | 0.71379 | 0.71742 | 0.71148 | 0.71890 | 0.70526 | 0.70515 | 0.70341 |
| 1.2 | 0.8 | 0.6 | 0.7 | 0.7 | 0.9 | 1.0 | 0.5 | 0.8 |
| 0.511678 ±20 | 0.511725 ±35 | 0.511679 ±27 | 0.511793 ±49 | 0.512052 ±25 | 0.511716 ±30 | 0.512224 ±31 | 0.512295 ±22 | 0.512916 ±20 |
| 0.1164 | 0.1150 | 0.1012 | 0.1157 | 0.1169 | 0.1263 | 0.1161 | 0.1063 | 0.1970 |
| -13.4 | -12.4 | -12.4 | -11.2 | -6.2 | -13.4 | -2.1 | -1.1 | 5.4 |
| 2.2 | 2.1 | 1.9 | 2.0 | 1.6 | 2.4 | 1.4 | 1.1 | 1.6 |

Craton as the principle source for the Cambrian sediments. Alternatively, by analogy with the interpretation of the Callanna and Sturtian sediments, renewed rifting may have resulted in uplift of rift-shoulders and preferential sampling of local basement material consistent with the turbiditic nature of the Kanmantoo Group. In either case, the Cambrian sediments lie within the basement envelopes on Fig. 7, allowing the possibility that they were derived purely by erosion of Gawler Craton material and their greater LREE-enrichment may imply a significant Archaean component. The Boxing Bay Formation, from the (?)upper Kanmantoo Group on Kangaroo Island, contains gneissic cobbles and has palaeocurrent directions (R. JENKINS, 1990, and pers. commun.) indicating derivation from basement material exposed on York Peninsula directly to the north (see Fig. 1) and the low $\epsilon$Nd of two Boxing Bay samples are quite consistent with this origin. If the Cambrian sediments were deposited in a foreland basin, a model which would resolve the restricted time-span between deposition and orogenesis, then either the emergent foreland did not contribute to the sediment package or else the foreland was similar, isotopically, to the Gawler Craton. This might be expected in an intra-continental fold belt where similar basement material would lie both to the east and west. Certainly, the inherited zircon data from the Lachlan Fold Belt granites demonstrates the existence of Proterozoic crust beneath eastern Australia (WILLIAMS et al., 1991). As noted earlier, it has been proposed that the Kanmantoo Group is allochthonous; however, the data presented here neither confirm nor disprove this hypothesis.

Finally, there is some evidence for a distinction between the Normanville/early Kanmantoo Group (Carrickalinga Formation) sediments, which have high $\epsilon$Nd and the subsequent Kanmantoo Group which have lower $\epsilon$Nd (Fig. 8b). The origin of this break is unclear but may indicate renewed emergence of the basement provenance region. Shales both before and after this break seem to show trends of decreasing $T_{DM}$ (Fig. 8b) and the pattern might be interpreted as episodic emergence of basement material. Overall the range of $\epsilon$Nd

Table 6. Geochemical and isotopic analyses of shales from Antarctica and the Glenelg River Complex and the lower Lachlan Fold Belt in Victoria

| *Stratigraphy* | *Wilson Terrane Antarctica* | *Wilson Terrane Antarctica* | *Glenelg River W Victoria* | *Glenelg River W Victoria* | *Glenelg River W Victoria* | *Monegeetta Shale* | *Lano Gully SST* |
|---|---|---|---|---|---|---|---|
| *Sample #* | *939-90-17* | *939-90-18* | *939-90-2* | *861-120* | *939-90-3* | *939-90-19* | *939-90-21* |
| *Lithology* | *schist* | *schist* | *And/schist* | *Gt/Bt schist* | *Gt/Bt schist* | *shale* | *siltstone* |
| *Locality* | *Berg Mts.* | *McCain Bluff* | *Wando River* | *Robertsons Ck.* | *Steep Bank R.* | *Kilmore Gap* | *Romsey* |
| *Est. Age (Ma)* | *?600* | *?600* | *527* | *527* | *527* | *500* | *490* |
| SiO2 | 72.12 | 57.92 | 62.21 | 56.58 | 62.04 | 73.54 | 73.88 |
| TiO2 | 0.64 | 0.87 | 0.91 | 1.01 | 1.11 | 0.76 | 0.67 |
| Al2O3 | 12.68 | 17.21 | 14.41 | 19.51 | 18.09 | 13.98 | 12.05 |
| Fe2O3 | 4.22 | 7.66 | 5.99 | 8.63 | 6.51 | 1.80 | 4.88 |
| MnO | 0.06 | 0.07 | 0.12 | 0.22 | 0.02 | 0.02 | 0.03 |
| MgO | 1.59 | 4.31 | 5.10 | 3.60 | 2.58 | 0.85 | 1.70 |
| CaO | 1.77 | 4.87 | 2.48 | 0.70 | 0.07 | 0.03 | 0.23 |
| Na2O | 2.92 | 1.60 | 1.65 | 1.72 | 0.22 | 0.05 | 1.53 |
| K2O | 3.00 | 3.53 | 2.74 | 5.54 | 3.74 | 3.44 | 2.43 |
| P2O5 | 0.20 | 0.22 | 0.43 | 0.15 | 0.16 | 0.11 | 0.19 |
| LOI | 0.44 | 1.41 | 3.51 | 2.01 | 4.74 | 4.09 | 2.41 |
| Total | 99.64 | 99.67 | 99.55 | 99.67 | 99.28 | 98.67 | 100.00 |
| Cr | 79 | 118 | 103 | 121 | 116 | 167 | 84 |
| Ni | 23 | 46 | 19 | 43 | 16 | 15 | 36 |
| Sc | 12 | 19 | 16 | 23 | 19 | 18 | 11 |
| V | 79 | 138 | 152 | 138 | 179 | 174 | 83 |
| Pb | 24 | 27 | 18 | 26 | 22 | 9 | 17 |
| Rb | 132.4 | 169.7 | 123.9 | 237.0 | 194.9 | 159.2 | 108.2 |
| Sr | 694.2 | 292.5 | 99.4 | 133.0 | 29.0 | 87.7 | 42.2 |
| Ba | 616 | 462 | 512 | 698 | 566 | 3945 | 1000 |
| Ga | 18 | 25 | 17 | | 23 | 19 | 15 |
| Nb | 13 | 16 | 14 | 22 | 16 | 15 | 12 |
| Zr | 261 | 142 | 191 | 185 | 176 | 141 | 232 |
| Y | 30 | 39 | 29 | 39 | 36 | 53 | 29 |
| Th | 20 | 16 | 10 | 24 | 14 | 16 | 10 |
| U | 1.4 | 3 | 3.4 | 6 | 3.5 | 9.9 | 3.6 |
| La | 42 | 41 | 41 | 49 | 48 | 58 | 40 |
| Ce | 87 | 76 | 66 | 104 | 89 | 127 | 78 |
| Nd | 39.78 | 38.07 | 28.17 | 22.70 | 43.08 | 56.14 | 35.80 |
| Sm | 7.48 | 7.72 | 6.11 | 4.28 | 8.38 | 10.55 | 6.91 |
| 87Sr/86Sr | 0.71770 ±4 | 0.72858 ±4 | 0.75237 ±8 | 0.75869 ±4 | 0.87253 ±9 | 0.75462 ±2 | 0.76642 ±9 |
| 87Rb/86Sr | 0.5525 | 1.6807 | 3.6090 | 5.1611 | 19.4989 | 5.2614 | 7.4336 |
| 87Sr/86Sr (t) | 0.71298 | 0.71420 | 0.72526 | 0.71993 | 0.72607 | 0.71713 | 0.71452 |
| TSr (DM) | 2.0 | 1.1 | 1.0 | 0.8 | 0.6 | 0.7 | 0.6 |
| 143Nd/144Nd | 0.511941 ±23 | 0.511940 ±32 | 0.511894 ±40 | 0.511796 ±27 | 0.511936 ±12 | 0.511851 ±19 | 0.511931 ±21 |
| 147Sm/144Nd | 0.1137 | 0.1227 | 0.1311 | 0.1141 | 0.1176 | 0.1137 | 0.1168 |
| eNd (t) | -7.2 | -8.0 | -10.2 | -11.0 | -8.5 | -10.1 | -8.8 |
| TNd (DM) | 1.7 | 1.9 | 2.2 | 2.0 | 1.8 | 1.9 | 1.8 |

values (−9.4 to −13.4) and trends of decreasing $T_{DM}$, shown by the Cambrian sediments, suggest mixing of basement material with more primitive detritus. This could be made from mantle derived volcanics such as the Truro volcanics that are intercalated with the Normanville Group (see Fig. 7). However, since these are of restricted occurrence and the higher $\epsilon$Nd sediments do not systematically contain higher Cr and Ni concentrations, mixing with re-cycled Adelaidean thermal-sag sediment, uplifted during renewed rifting, is postulated instead.

## Gondwanan Correlations

As part of on-going research, especially on equivalent sedimentary sequences in Tasmania (J. D. Foden, work in progress), data were collected on sediments from the Glenelg River Complex in western Victoria and the Wilson Terrane in Antarctica (see Table 6) as a means of assessing the Gondwanan correlations outlined at the beginning of this paper. On the basis of their similar bulk rock and isotope chemistry, the shales from the Glenelg River Complex can be well correlated with those of the Adelaide Fold Belt; however, the present data is insufficient to distinguish which of the Adelaidean or Kanmantoo/Normanville provide the best correlation. In contrast, the two samples from the Wilson Terrane have $\epsilon$Nd of −7 and −8, and therefore correlate best with the Adelaidean sequences consistent with structural correlations discussed by FLÖTTMANN and KLEINSCHMIDT (1991).

YOUNG (1992) has recently proposed a correlation between the Windermere Supergroup in NW Canada and the Umberatana-Wilpena Groups of the Adelaidean. Neodymium isotopic data from the Windermere Supergroup in British Columbia (BURWASH et al., 1988) show high average model ages (~2.3 Ga) and generally low $\epsilon$Nd (−6 to −18 at 700 Ma) that do not appear to correlate with the Adelaidean thermal-sag-phase sediments. This data either requires different provenance regions for the two or a greater Archaean source input for the Windermere Supergroup.

Table 6. (*Continued*)

| *Darraweit MS* | *Graptolite Shale* | *itate Circle Shale* |
|---|---|---|
| *939-90-20 mudstone Darraweit* | *939-90-4 Shale Bendigo shale* | *939-90-12 Shale shale* |
| *440* | *460* | *440* |
| 33.09 | 66.36 | 67.99 |
| 0.41 | 0.77 | 0.63 |
| 10.90 | 17.33 | 14.25 |
| 3.48 | 5.20 | 6.60 |
| 0.04 | 0.07 | 0.07 |
| 2.19 | 0.90 | 2.23 |
| 24.05 | 0.01 | 0.25 |
| 0.04 | 0.28 | 0.20 |
| 2.74 | 3.93 | 3.44 |
| 0.10 | 0.02 | 0.08 |
| 22.20 | 4.05 | 4.32 |
| 99.24 | 98.92 | 100.06 |
| 102 | 115 | 157 |
| 35 | 56 | 57 |
| 11 | 12 | 13 |
| 94 | 692 | 135 |
| 10 | 17 | 9 |
| 141.1 | 232.3 | 147.7 |
| 711.3 | 39.7 | 42.2 |
| 1771 | 1039 | 529 |
| 14 | 23 | 19 |
| 9 | 15 | 12 |
| 65 | 144 | 140 |
| 22 | 30 | 29 |
| 19 | 14 | 14 |
| 1.5 | 6.9 | 1.5 |
| 24 | 65 | 42 |
| 47 | 101 | 76 |
| 24.40 | 36.70 | 32.64 |
| 4.75 | 6.45 | 6.12 |
| 0.71773 ±5 | 0.82421 ±5 | 0.77718 ±5 |
| 0.5745 | 16.9329 | 10.1449 |
| 0.71413 | 0.71324 | 0.71359 |
| 1.9 | 0.5 | 0.5 |
| 0.511875 ±23 | 0.511796 ±36 | 0.511843 ±31 |
| 0.1178 | 0.1064 | 0.1135 |
| -10.5 | -11.1 | -10.8 |
| 1.9 | 1.8 | 1.9 |

## Sediments of the Lachlan Fold Belt

The turbiditic shales from the Lachlan Fold Belt have εNd values that overlap those of the Adelaidean and Cambrian successions of the Adelaide Fold Belt to the west, and this would be quite consistent with their being reworked detritus eroded from a Delamerian mountain range, probably with some input from the isotopically more primitive Delamerian intrusives (Table 5; Fig. 7). Such a hypothesis can be evaluated, to some extent, by looking for compositional evidence of weathering, as outlined in the following text.

Various studies have shown that, during sedimentary cycles, $Na_2O$ is preferentially removed into seawater and CaO taken up in carbonates. Consequently, reworked sediments have higher $K_2O/Na_2O$ ratios than their precursors. NESBITT and YOUNG (1982) defined a chemical index of alteration $CIA = [Al_2O_3/(Al_2O_3 + CaO + Na_2O + K_2O)] \times 100$ with increased weathering resulting in higher values. Similarly, HARNOIS (1988) proposed a chemical index of weathering $CIW = [Al_2O_3/(Al_2O_3 + CaO + Na_2O)] \times 100$ with increased alteration leading to higher values. Average values of these parameters for the basement material and Adelaidean, Kanmantoo/Normanville, and Lachlan Fold Belt shales are listed in Table 8. The basement values are uniformly the lowest and it can be seen that the Lachlan Fold belt shales have values much higher than either the Adelaidean or Kanmantoo/Normanville shales which are themselves intermediate between the basement and the Lachlan Fold Belt shales. This is consistent with the turbiditic Lachlan Fold Belt sediment sequence representing reworked and redeposited material from the Adelaide Fold Belt—a notion supported by the presence of detrital zircons of Late Proterozoic to Cambro-Ordovician age in these sediments (WILLIAMS et al., 1991). The Bendigo shale has a higher $La/Yb_N$ than either the Adelaidean or Kanmantoo/Normanville and this LREE-enrichment may reflect recycling (e.g., NESBITT et al., 1990; ZHAO et al., 1992).

We note in passing that the average Kanmantoo/Normanville shale has lower $K_2O/Na_2O$ and CIW ratios than

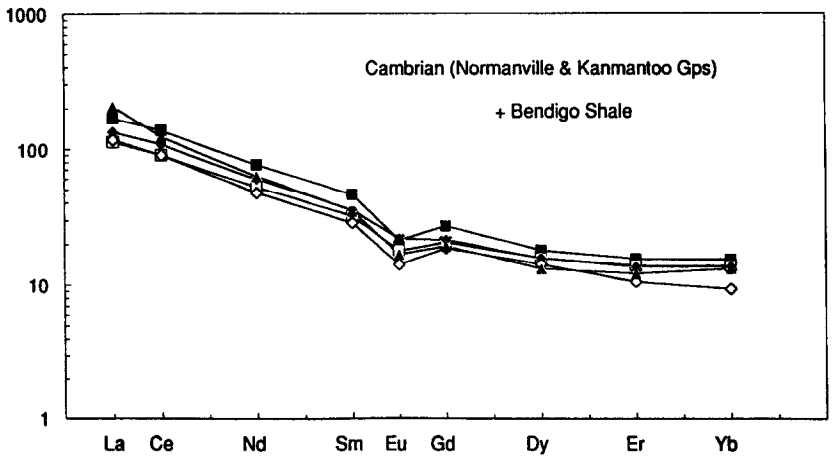


FIG. 6. Chondrite-normalized rare earth patterns for selected Cambrian shales: Sellick Hill Formation shale (filled squares); Carrickalinga Formation shale (open squares); Tappanappa Formation shale (filled diamonds); Petrel Cove Formation shale (open diamonds). Also plotted is the Ordovician shale from Bendigo in the Lachlan Fold Belt (filled triangles).

Table 7. Rare earth analyses of selected lithologies from Tables 2-6.

| Sample # | La | Ce | Nd | Sm | Eu | Gd | Dy | Er | Yb |
|---|---|---|---|---|---|---|---|---|---|
| 446/256 | 88.30 | 214.64 | 96.63 | 16.16 | 1.06 | 7.49 | 3.41 | 1.24 | 0.84 |
| 446/C142 | 6.58 | 16.92 | 8.12 | 2.32 | 0.65 | 2.86 | 3.86 | 2.35 | 2.43 |
| 6131RS14 | 51.58 | 130.48 | 50.70 | 8.88 | 1.93 | 5.83 | 3.03 | 0.82 | 0.45 |
| 515-B26 | 23.90 | 50.90 | 23.30 | 4.48 | 1.28 | 4.47 | 4.22 | 2.68 | 2.67 |
| 515-B143 | 58.50 | 120.00 | 50.90 | 9.58 | 1.77 | 8.60 | 7.93 | 4.62 | 4.32 |
| 515-B152 | 39.00 | 74.00 | 33.80 | 5.74 | 0.16 | 6.45 | 7.13 | 4.33 | 4.02 |
| 6131RS747 | 17.25 | 52.59 | 16.68 | 3.61 | 0.79 | 3.32 | 4.09 | 2.79 | 3.15 |
| 939-90-14 | 41.01 | 75.75 | 29.20 | 5.38 | 0.87 | 4.85 | 4.43 | 2.67 | 2.85 |
| RS27 | 6.32 | 17.71 | 12.91 | 3.94 | 1.35 | 4.73 | 5.19 | 2.96 | 2.78 |
| W6 | 9.40 | 23.54 | 15.47 | 4.34 | 1.65 | 4.89 | 4.90 | 2.69 | 2.35 |
| 939-90-8 | 23.42 | 61.68 | 16.87 | 2.94 | 0.56 | 3.30 | 2.81 | 1.46 | 2.01 |
| 939-90-7 | 29.01 | 61.78 | 28.46 | 5.95 | 1.19 | 5.48 | 5.15 | 3.00 | 2.84 |
| 814-041-53 | 32.00 | 72.71 | 31.09 | 6.11 | 1.02 | 4.97 | 4.43 | 2.38 | 2.33 |
| 819-18 | 38.38 | 75.54 | 33.58 | 6.69 | 1.27 | 5.39 | 5.34 | 3.05 | 2.96 |
| 819-84 | 48.01 | 89.61 | 44.08 | 9.52 | 1.95 | 8.43 | 7.78 | 4.28 | 4.28 |
| 939-90-5 | 52.64 | 112.39 | 46.09 | 8.96 | 1.56 | 7.05 | 5.93 | 3.34 | 3.23 |
| 876-1013 | 111.80 | 179.27 | 75.16 | 12.36 | 3.81 | 9.84 | 7.22 | 3.26 | 2.52 |
| 876-1017 | 35.96 | 74.37 | 31.53 | 6.43 | 1.30 | 5.35 | 5.18 | 2.98 | 2.89 |
| 474-R40 | 42.05 | 88.91 | 36.02 | 6.95 | 1.59 | 5.60 | 5.16 | 2.92 | 2.85 |
| 474-CN1 | 36.88 | 74.19 | 28.46 | 5.59 | 1.02 | 4.84 | 4.63 | 2.24 | 1.94 |
| 779-52 | 14.89 | 25.78 | 10.81 | 1.98 | 1.08 | 1.92 | 1.53 | 0.79 | 0.75 |
| 861-93 | 79.93 | 155.36 | 59.89 | 10.53 | 1.67 | 8.60 | 8.90 | 5.17 | 5.29 |
| 898-350 | 3.24 | 7.81 | 5.77 | 1.88 | 0.78 | 2.62 | 3.18 | 1.93 | 1.90 |
| 939-90-4 | 64.55 | 101.43 | 37.99 | 6.83 | 1.22 | 5.03 | 4.31 | 2.58 | 2.76 |

the average for the Adelaidean shales, supporting the notion that these sediments involved material derived from the basement and were not derived by backstripping of the Adelaidean alone.

## Lithospheric Evolution

The lithological sequences previously described can be broken into three principle episodes: the Archaean leading up to the Sleafordian Orogeny; the Early- to Mid-Proterozoic including the Kimban Orogeny; and the Late Proterozoic to Cambrian sedimentary history of the Adelaide Fold Belt, culminating in the Delamerian Orogeny. New mantle additions to the crust are manifested by mafic magmatism in each of these episodes, and many of the accompanying felsic magmatic rocks have quite primitive isotopic characteristics that suggests they also contain a mantle component and are not simply recycled pre-existing crust. The magmatic rocks of the Delamerian Orogeny (see Fig. 7; Table 5) are notably all far more primitive isotopically than either the basement or the sediments. This implies a major role for mantle derived material during the Delamerian Orogeny—a conclusion also reached through considerations of the thermal implications of metamorphism and deformation (SANDIFORD et al., 1992).

Much of the isotopic variation within the Adelaidean and Kanmantoo/Normanville sequences is interpreted as a response to changes in provenance size and episodic rift-shoulder development. Nevertheless, both of these sequences show isotopic trends implying mixing between the older Gawler Craton basement material and a more primitive source. Ad-

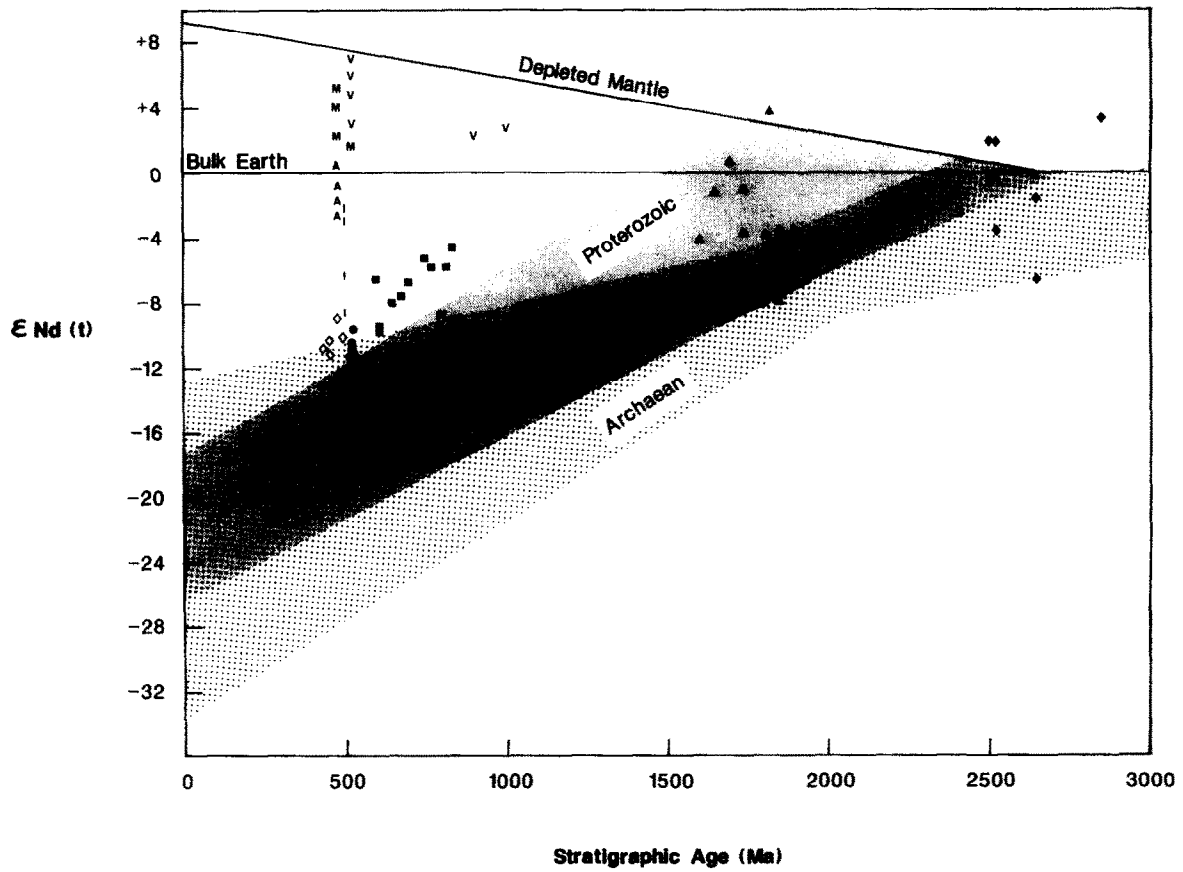


FIG. 7. εNd evolution diagram for the Gawler Craton basement (Archaean = filled diamonds, Early- and Mid-Proterozoic = filled triangles), the Adelaidean shales (filled squares), the Cambrian Normanville and Kanmantoo Group shales including three sediments from the Glenelg River Complex (filled circles) and Cambrian and Ordovician shales from the Lachlan Fold Belt (open diamonds). Also plotted are samples of the Gairdner Dyke Swarm and Wooltana Volcanics (V's at the base of the Adelaidean), the Truro Volcanics (V's at the base of the Cambrian) and various Delamerian mafic magmatic rocks (M's), I-type granites (I's), an S-type granite (S) and late-orogenic A-type granites (A's). The depleted mantle evolution curve is essentially that used by ALBARÈDE and BROUXEL (1987). The coarse stipple represents the evolution envelope for the Archaean samples and the light grey stipple that for the Early- and Mid-Proterozoic ones (see text for explanation).

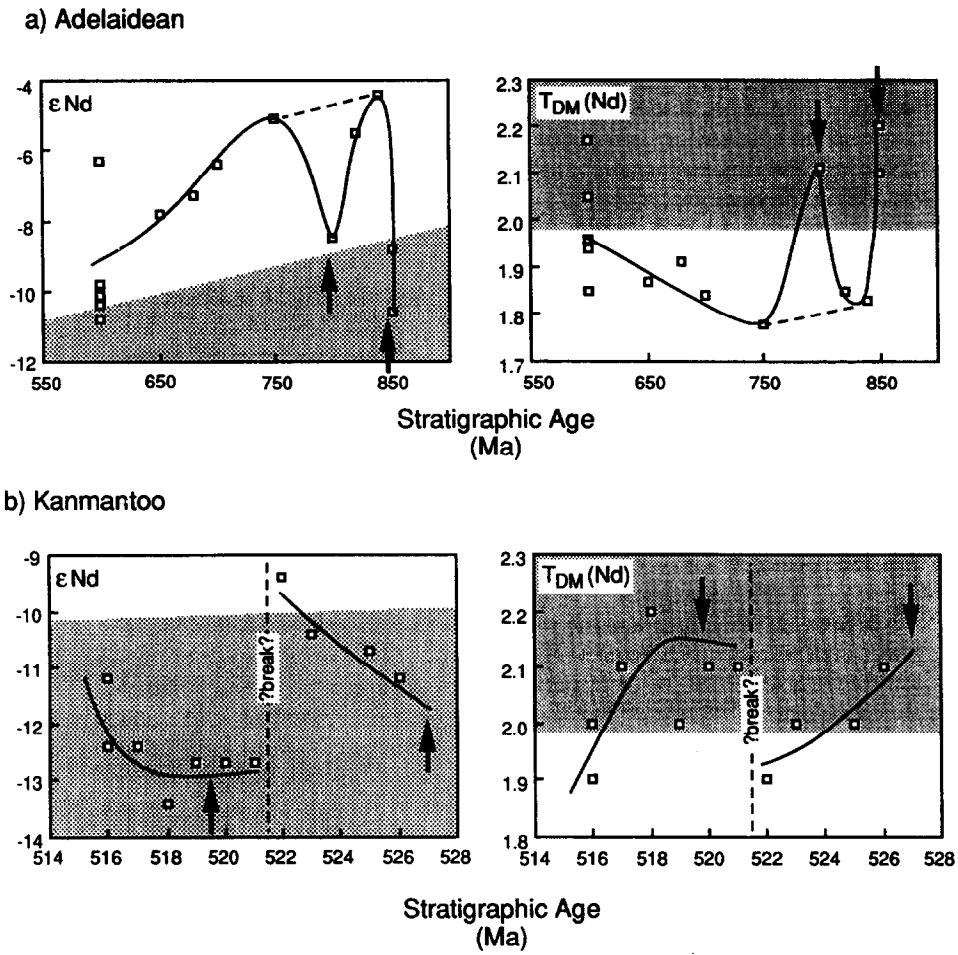


FIG. 8. $\epsilon$Nd and depleted mantle model age vs. stratigraphic age for the Adelaidean and Normanville/Kanmnatoo sequences. The stipple shows the position of the bulk Gawler Craton basement and the arrows indicate possible basement emergence episodes. (a) Adelaidean sequences. The early rift-phase sediments have low $\epsilon$Nd and high $T_{DM}$ consistent with derivation from the local basement whereas the sag-phase sediments do not, reflecting the averaging of a much larger provenance region. This signature gradually decays towards lower $\epsilon$Nd and higher $T_{DM}$ as erosion excavates deeper levels of the provenance region. Note the divergence of the Sturtian tillite back to rift-phase values possibly indicating the rise of rift-shoulders (see text for explanation). (b) Kanmantoo/Normanville sequences. These show $\epsilon$Nd and $T_{DM}$ values consistent with derivation from the basement. Note the apparent division of the sequence at 521 Ma into two sets which show trends of mixing or provenance change with time.

ditionally, there is good evidence for contemporary mafic volcanism, at the beginning of the Adelaidean and in the upper Normanville Group. Even though our calculations suggest these volcanics are unlikely to represent the primitive endmember, it seems clear that mantle additions to the crust occurred during both episodes of extension and sedimentation, and also during orogenesis. This is supported by evidence for an episodic formation of the lower crust and upper mantle in South Australia. Zircon ages (CHEN et al., 1992) from xenoliths from kimberlite pipes cluster around: 1700–1400 Ma (Kimban-Wartakan orogeny); 800–700 Ma (Adelaidean thermal-sag-phase); and 530–480 Ma (Delamerian Orogeny).

Table 8. Average weathering parameters for shales and Gawler Craton basement material.

| *Parameter* | *Archaean* | *Early to Mid-Proterozoic* | *Adelaidean* | *Kanmantoo/ Normanville* | *Lachlan Fold Belt* |
|---|---|---|---|---|---|
| K2O/Na2O | 0.9 | 1.9 | 4.6 | 2.8 | 34.1 |
| CIA | 61 | 60 | 65 | 65 | 68 |
| CIW | 69 | 73 | 80 | 76 | 83 |

The discussion so far leads to a model for progressive crustal additions on the regional scale and largely in an intra-continental rather than continental margin setting. This contrasts with subsequent Palaeozoic continental additions which largely took the form of marginal accretion. Of course, a model for crustal additions on the regional scale is only a first order step in constraining the question of continuous crustal growth vs. the steady state model on a global scale since this additionally requires an assessment of the rate of recycling of crustal material back into the mantle (e.g., ARMSTRONG, 1991). Comparison of the depleted mantle model ages and stratigraphic ages for the samples analysed in this study (Fig. 9) shows that Sr model ages tend to approximate the stratigraphic age whilst the Nd model ages diverge from this concordance at about 2 Ga and thereafter level out at 1.8 Ga. This has been observed by other workers (e.g., MILLER et al., 1986; GOLDSTEIN, 1988) but again, does not help to constrain crustal growth models (ARMSTRONG, 1991). One important observation is the occurrence of Gawler Craton Archaean rocks that lie above the depleted mantle curve with positive $\epsilon$Nd (Fig. 7). Similar data have been reported in other studies (e.g., MCCULLOCH and COMPSTON, 1981; SMITH and LUDDEN, 1989; SIVELL and MCCULLOCH, 1991) and because of the slow decay rate of $^{147}Sm$ to $^{143}Nd$ these require that a depleted mantle reservoir must have been in existence very early in earth history.

With the exception of the Archaean basaltic dykes, the ubiquitous LREE-enrichment (comparable to the post Archaean average shale of TAYLOR and MCLENNAN, 1985) of the shales and igneous rocks analyzed in this study brings to question the mechanism of continental crust formation. As shown by O'NIONS and MCKENZIE (1988), the LREE-enrichment of such patterns requires that a small melt fraction be involved at some stage in the generation of continental crust and this may form a low melting temperature zone within the lithospheric mantle (MCKENZIE, 1989). Access of this material requires a perturbation in the thermal structure of the lithosphere as will occur during extension or orogenesis. In general our data point to local crustal additions during these episodes of extension and orogenesis and favour crustal assimilation by mantle magmas rather than intra-crustal recycling.

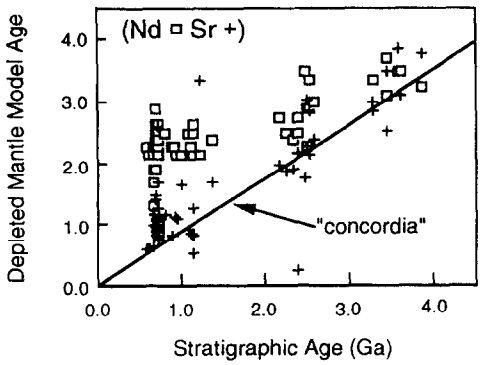


FIG. 9. Plot of Sr($T$Sr(DM)) and Nd($T$Nd(DM)) depleted mantle model ages against stratigraphic age showing the tendency for Sr model ages to approximate stratigraphic ages whilst Nd model ages depart from this concordance and level out at around 1.8 Ga.

## SUMMARY AND CONCLUSIONS

Whole rock geochemistry and isotopes, in particular $\epsilon$Nd values, have been successfully used to characterize and investigate the geological history of the Adelaide Fold Belt. As part of an ongoing investigation we can presently make the following conclusions:

1) The Archaean to Mid-Proterozoic Gawler Craton basement in South Australia records a history of additions from the contemporary depleted mantle, some of which assimilated pre-existing crust.
2) The Adelaidean sedimentary sequences of the Adelaide Fold Belt may be resolved into a rift-phase followed by a thermal-sag-phase. They are not simply composed of detritus eroded from this basement and contain a significant component from a more juvenile source. Periods of rift-shoulder development are marked by increased restriction of the sediment source to the basement.
3) The Sturtian glaciogenic sediments may reflect the development of rift-shoulders.
4) The Normanville and Kanmantoo Group sediments differ from the preceding Adelaidean in that they may have been derived from the basement, which may have become emergent due to renewed rifting, along with some reworking of Adelaidean material.
5) Preliminary data suggest that sediments from the Wilson Terrane in Antarctica correlate well with the Adelaidean; however those from the Glenelg River Complex may match either the Adelaidean of the Kanmantoo Group. If the Adelaidean sequences and the Windemere Supergroup in Canada can be correlated, they either have different sources or different relative source contributions.
6) The chemical and isotopic data are consistent with a mode in which deformation and subsequent rapid exhumation during the Delamerian Orogeny provided the source for the thick Ordovician-Silurian flysch in the Lachlan Fold Belt to the east.
7) The data indicate a model of regional, intra-continental additions via advection of mantle melts accompanied by assimilation of pre-existing crustal materials. They do not support one of purely intra-crustal recycling.
8) This model does not constrain the debate over continuous vs steady state crustal growth, though positive $\epsilon$Nd values for Archaean samples require the presence of a depleted mantle source early in the Earth's history.

*Acknowledgments*—Many people have made useful suggestions and supplied samples or data either directly or through unpublished theses. The early results of this work were presented at the 11th Australian Geological Convention at Ballarat in January 1992 where many people offered further samples and helpful advice. All of these people deserve thanks; however, Richard Flint, Nick Lemon, Malcom Wallace, Fonz Vandenberg, Vic Gostin, Reid Keays, and Thomas Flöttmann are specifically thanked for supplying samples. Thanks also go to Nick Lemon, Vic Gostin, Richard Jenkins and Peter Haines for their various suggestions and advice on stratigraphic ideas. Carol Frost, Ann Linn, and Grant Young are particularly thanked for thoughtful reviews which helped to improve the paper.

*Editorial handling*: S. M. McLennan

## REFERENCES


ALBARÈDE F. and BROUXEL M. (1987) The Sm/Nd secular evolution of the continental crust and the depleted mantle. *Earth Planet. Sci. Lett.* **82**, 25–35.

ALLÈGRE C. J. (1982) Chemical geodynamics. *Tectonophysics* **81**, 109–132.

ALLÈGRE C. J. and ROUSSEAU D. (1984) The growth of the continent through geological time studied by Nd isotope analysis of shales. *Earth Planet. Sci. Lett.* **67**, 19–34.

ARMSTRONG R. L. (1981) Radiogenic isotopes: The case for crustal recycling on a near-steady-state no-continental-growth Earth. *Phil. Trans. Roy. Soc. London* **A301**, 443–472.

ARMSTRONG R. L. (1991) The persistent myth of crustal growth. *Aust. J. Earth. Sci.* **38**, 613–630.

ARNDT N. T. and GOLDSTEIN S. L. (1987) Use and abuse of crust formation ages. *Geology* **15**, 893–895.

AWWILLER D. N. and MACK L. E. (1991) Diagenetic modification of Sm-Nd model ages in Tertiary sandstones and shales, Texas Gulf Coast. *Geology* **19**, 311–314.

BALLIE P. W. (1985) A Palaeozoic suture in eastern Gondwanaland. *Tectonics* **4**, 653–660.

BURWASH R. A., CAVELL P. A., and BURWASH E. J. (1988) Source terranes for Proterozoic sedimentary rocks in southern British Columbia: Nd isotopic and petrographic evidence. *Canadian J. Earth Sci.* **25**, 824–832.

CAS R. (1983) Palaeogeographic and tectonic development of the Lachlan Fold Belt southeastern Australia. *Geol. Soc. Aust. Spec. Publ.* **10**.

COATS R. P. (1981) Late Proterozoic (Adelaidean) tillites of the Adelaide Geosyncline, In *Earth's pre-Pleistocene glacial record.* (ed. M. J. HAMBREY and W. B. HARLAND), pp. 537–548. Cambridge Univ. Press.

CHEN Y. D., O'REILLY S. Y., and KINNY P. (1992) Dating the cratonic lower crust by SHRIMP: A U-Th-P isotopic study on zircons from lower crustal xenoliths from kimberlite pipes. *Geol. Soc. Aust. Abst.* **32**, 215–216.

COOPER J. A., JENKINS R. J. F., COMPSTON W., and WILLIAMS I. S. (1992) Ion-probe zircon dating of a mid-Early Cambrian tuff in South Australia. *J. Geol. Soc. London* **149**, 185–192.

CRAWFORD A. J. and HILYARD D. (1990) Geochemistry of Late Proterozoic tholeiitic flood basalts, Adelaide Geosyncline, South Australia. *Geol. Soc. Aust. Spec. Publ.* **16**, 49–67.

CROCK J. G., LICHTE F. E., and WILDMAN T. R. (1984) The group separation of the rare-earth elements and yttrium from geologic materials by cation-exchange chromatography. *Chem. Geol.* **45**, 149–163.

DAILY B., FIRMAN J. B., FORBES B. G., and LINDSAY J. M. (1976) Geology. In *Natural History of the Adelaide Region* (ed. C. R. TWIDALE et al.), pp. 17–18. Roy. Soc. S. Aust.

DEWEY J. F. and WINDLEY B. F. (1981) Growth and differentiation of the continental crust. *Phil. Trans. Roy. Soc. London* **A301**, 189–206.

FANNING C. M. (1975) Petrology, structure and geochronology of some high grade metamorphic rocks at Fishery Bay and Cape Carnot, Southern Eyre Peninsula. Hons. Thesis, Univ. Adelaide.

FANNING C. M., FLINT R. B., PARKER A. J., LUDWIG K. R., and BLISSETT A. H. (1988) Refined Proterozoic evolution of the Gawler Craton, South Australia, through U-Pb zircon geochronology. *Precambrian Res.* **40/41**, 363–386.

FODEN J. D., TURNER S. P., and MORRISON R. S. (1990) The tectonic implications of Delamerian magmatism in South Australia and western Victoria. *Geol. Soc. Aust. Spec. Publ.* **16**, 465–482.

FODEN J. D., TURNER S. P., and MICHARD A. (1993a) Late Proterozoic and early Palaeozoic crustal development in South Australia and Tasmania: Implications based on Nd- and Sr-isotopic results. (In prep).

FODEN J. D., TURNER S. P., SANDIFORD M., WILLIAMS I. S., COMPSTON W., and MICHARD A. (1993b) The nature, timing and duration of the Delamerian-Ross Orogeny. *J. Geol. Soc. London* (submitted).

FORBES B. G., COATS R. P., and DAILY B. (1972) Truro volcanics. *Quarterly Geological Notes, Geol. Surv. S. Aust.* **44**, 1–5.

FLÖTTMANN T. and KLEINSCHMIDT G. (1991) Opposite thrust systems in northern Victoria Land, Antarctica: Imprints of Gendwana's Palaeozoic accretion. *Geology* **19**, 45–47.

FROST C. D. and WINSTON D. (1987) Nd isotope systematics of coarse- and fine-grained sediments: Examples from the Middle Proterozoic Belt-Purcell Supergroup. *J. Geol.* **95**, 309–327.

GOLDSTEIN S. L. (1988) Decoupled evolution of Nd and Sr isotopes in the continental crust and the mantle. *Nature* **336**, 733–738.

GOSTIN V. A., HAINES P. W., JENKINS R. J. F., COMPSTON W., and WILLIAMS I. S. (1986) Impact ejecta horizon within Late Precambrian shales, Adelaide Geosyncline, South Australia. *Science* **223**, 189–200.

HARNOIS L. (1988) The CIW Index: A new chemical index of weathering. *Sediment. Geol.* **55**, 319–322.

JENKINS R. J. F. (1986) Ralph Tate's enigma and the regional significance of thrust faulting in the Mt Lofty Ranges. *Geol. Soc. Aust. Abstr.* **15**, 101.

JENKINS R. J. F. (1990) The Adelaide Foldbelt: Tectonic reappraisal. *Geol. Soc. Aust. Spec. Publ.* **16**, 396–420.

LAIRD M. G. and GRINDLEY G. W. (1982) Antarctica. *Geol. Soc. Aust. Spec. Publ.* **9**, 17–22.

MANCKTELOW N. S. (1979) The structure and metamorphism of the southern Adelaide Fold Belt. Ph.D. thesis, Univ. Adelaide.

MCCULLOCH M. T. (1987) Sm-Nd isotopic constraints on the evolution of Precambrian crust in the Australian continent. In *Proterozoic Lithospheric Evolution.* (ed. A. KRONER), pp. 115–130. *Amer. Geophys. Uni. Geodynamics Series* **17**.

MCCULLOCH M. T. and COMPSTON W. (1981) Sm-Nd age of Kambalda and Kanowna greenstones and heterogeneity in the Archaean mantle. *Nature* **294**, 322–327.

MCCULLOCH M. T. and WASSERBURG G. J. (1978) Sm-Nd and Rb-Sr chronology of continental crust formation. *Science* **200**, 1003–1011.

MCKENZIE D. (1978) Some remarks on the development of sedimentary basins. *Earth Planet. Sci. Lett.* **40**, 25–32.

MCKENZIE D. (1989) Some remarks on the movement of small melt fractions in the mantle. *Earth Planet. Sci. Lett.* **95**, 53–72.

MCLENNAN S. M., MCCULLOCH M. T., TAYLOR S. R., and MAYNARD J. B. (1989) Effects of sedimentary sorting on neodymium isotopes in deep-sea turbidities. *Nature* **337**, 547–549.

MILLER R. G., O'NIONS R. K., HAMILTON P. J., and WELIN E. (1986) Crustal residence ages of clastic sediments, orogeny and continental evolution. *Chem. Geol.* **57**, 87–99.

MORTIMER G. E. (1984) Granitoids and basaltic dykes, southern Eyre Peninsula. Ph.D. thesis, Univ. Adelaide.

NESBITT H. W. and YOUNG G. M. (1982) Early Proterozoic climates and plate motions inferred from the major element chemistry of lutites. *Nature* **299**, 715–717.

NESBITT H. W., MACRAE N. D., and KROUBERG, B. I. (1990) Amazon deep-sea fan muds: Light REE enriched products of extreme chemical weathering. *Earth. Planet. Sci. Lett.* **100**, 118–123.

O'NIONS R. K. and MCKENZIE D. P. (1988) Melting and continent generation. *Earth Planet. Sci. Lett.* **90**, 449–456.

PREISS W. V. (1987) The Adelaide Geosyncline-Late Proterozoic stratigraphy, sedimentation, palaeontology and tectonics. *Bull. Geol. Surv. S. Australia* **53**.

REYMER A. and SCHUBERT G. (1984) Phanerozoic addition rates to the continental crust and crustal growth. *Tectonics* **3**, 63–77.

RICHARD P., SHIMIZU N., and ALLÈGRE C. J. (1976) $^{143}Nd/^{144}Nd$, a natural tracer: An application to oceanic basalts. *Earth Planet. Sci. Lett.* **31**, 269–278.

SANDIFORD M., OLIVER R. L., MILLS K. J., and ALLEN R. V. (1990) A cordierite-staurolite-muscovite association, east of Springton, Mt Lofty Ranges; Implications for the metamorphic evolution of the Kanmantoo Group. *Geol. Soc. Aust. Spec. Publ.* **16**, 483–495.

SANDIFORD M., FODEN J., ZHOU S., and TURNER S. (1992) Granite genesis and the mechanics of convergent orogenic belts with application to the Southern Adelaide Fold Belt. *Trans. Roy. Soc. Edinburgh.* **83**, 83–93.

SIVELL W. J. and MCCULLOCH M. T. (1991) Neodymium isotope evidence for ultra-depleted mantle in the early Proterozoic. *Nature* **354**, 384–387.

SMITH A. D. and LUDDEN J. N. (1989) Neodymium isotopic evo-

lution of the Precambrian mantle. *Earth Planet. Sci. Lett.* **93,** 14–22.

SUN S-S. and NESBITT R. W. (1978) Petrogenesis of Archaean ultrabasic and basic volcanics: Evidence from rare earth elements. *Contrib. Mineral. Petrol.* **65,** 301–325.

TAYLOR S. R. and MCLENNAN S. M. (1985) *The Continental Crust: Its Composition and Evolution.* Blackwell.

THOMPSON B. P. (1969) The Kanmantoo Group and Early Palaeozoic tectonics. In *Handbook of South Australian Geology* (ed. L. W. PARKIN), pp. 97–108. Geol. Surv. S. Aust.

TURNER S. P. (1991) Late-orogenic, mantle-derived bimodal magmatism in the southern Adelaide Foldbelt, South Australia. Ph.D. thesis, Univ. Adelaide.

TURNER S. P. and FODEN J. D. (1990) The nature of mafic magmatism through the evolution of the Adelaide Foldbelt and subsequent Delamerian Orogeny. In *Mafic Dykes and Emplacement Mechanisms.* (ed. A. J. PARKER et al.), pp. 431–434. Balkema.

TURNER S. P., FODEN J. D., and MORRISON R. S. (1992a) Derivation of some A-type magmas by fractionation of basaltic magma and an example from the Padthaway Ridge, South Australia. *Lithos* **28,** 151–179.

TURNER S. P., ADAMS C. J., FLÖTTMANN T., and FODEN J. D. (1992b) Geochemical and geochronological constraints on the Glenelg River Complex, western Victoria. *Aust. J. Earth Sci.* (in press).

VAN DER STELT B. J. (1990) The geochemistry, petrology and tectonic setting of the Truro Volcanics. Hons. thesis, Univ. Adelaide.

VON DER BORCH C. C. (1980) Evolution of Late Proterozoic to Early Palaeozoic Adelaide Foldbelt, Australia: Comparisons with post-Permian margins. *Tectonophysics* **70,** 115–134.

WEAVER B. L. and TARNEY J. (1981) Lewisian gneiss geochemistry and Archaean crustal development models. *Earth Planet. Sci. Lett.* **55,** 171–180.

WEBB A. B., THOMSON B. P., BLISSETT A. H., DALY S., FLINT R. B., and PARKER A. J. (1986) Geochronology of the Gawler Craton, South Australia. *Aust. J. Earth Sci.* **33,** 119–143.

WILLIAMS E. (1978) Tasman Fold Belt system in Tasmania. *Tectonophysics* **48,** 159–205.

WILLIAMS I. S., CHAPPELL B. W., CHEN Y. D., and CROOK K. A. W. (1991) Inherited and detrital zircons—vital clues to the granite protoliths and early igneous history of southeastern Australia. Second Granites Conference, BMR record 1991/25.

YOUNG G. M. (1992) Late Proterozoic stratigraphy and the Canada-Australia connection. *Geology* **20,** 215–218.

YOUNG G. M. and GOSTIN V. A. (1988) Stratigraphy and sedimentology of Sturtian glaciogenic deposits in the western part of the North Flinders Basin, South Australia. *Precambrian Res.* **39,** 151–170.

ZHAO J. X., MCCULLOCH M. T., and BENNETT V. C. (1992) Sm-Nd and U-Pb zircon isotopic constraints on the provenance of sediments from the amadeus Basin, central Australia: Evidence for REE fractionation. *Geochim. Cosmochim. Acta.* **56,** 921–940.